Figure 3

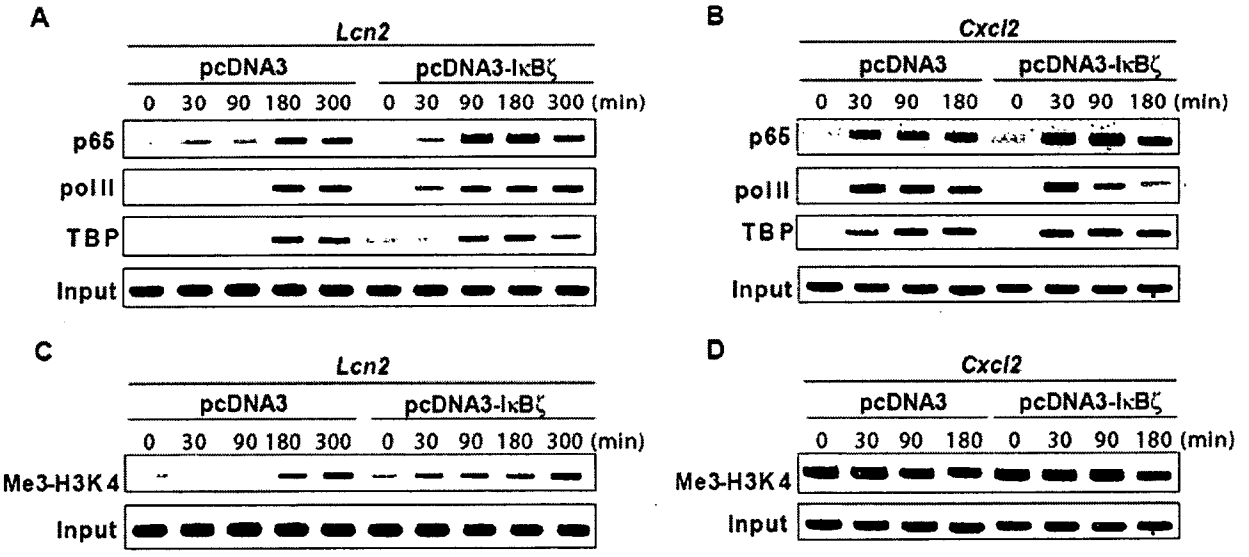
A
Lcn2
pcDNA3
pcDNA3-IκBζ
0 30 90 180 300 0 30 90 180 300 (min)
p65
polII
TBP
Input
B
Cxcl2
pcDNA3
pcDNA3-IκBζ
0 30 90 180 0 30 90 180 (min)
p65
polII
TBP
Input
C
Lcn2
pcDNA3
pcDNA3-IκBζ
0 30 90 180 300 0 30 90 180 300 (min)
Me3-H3K4
Input
D
Cxcl2
pcDNA3
pcDNA3-IκBζ
0 30 90 180 0 30 90 180 (min)
Me3-H3K4
Input

Figure 4

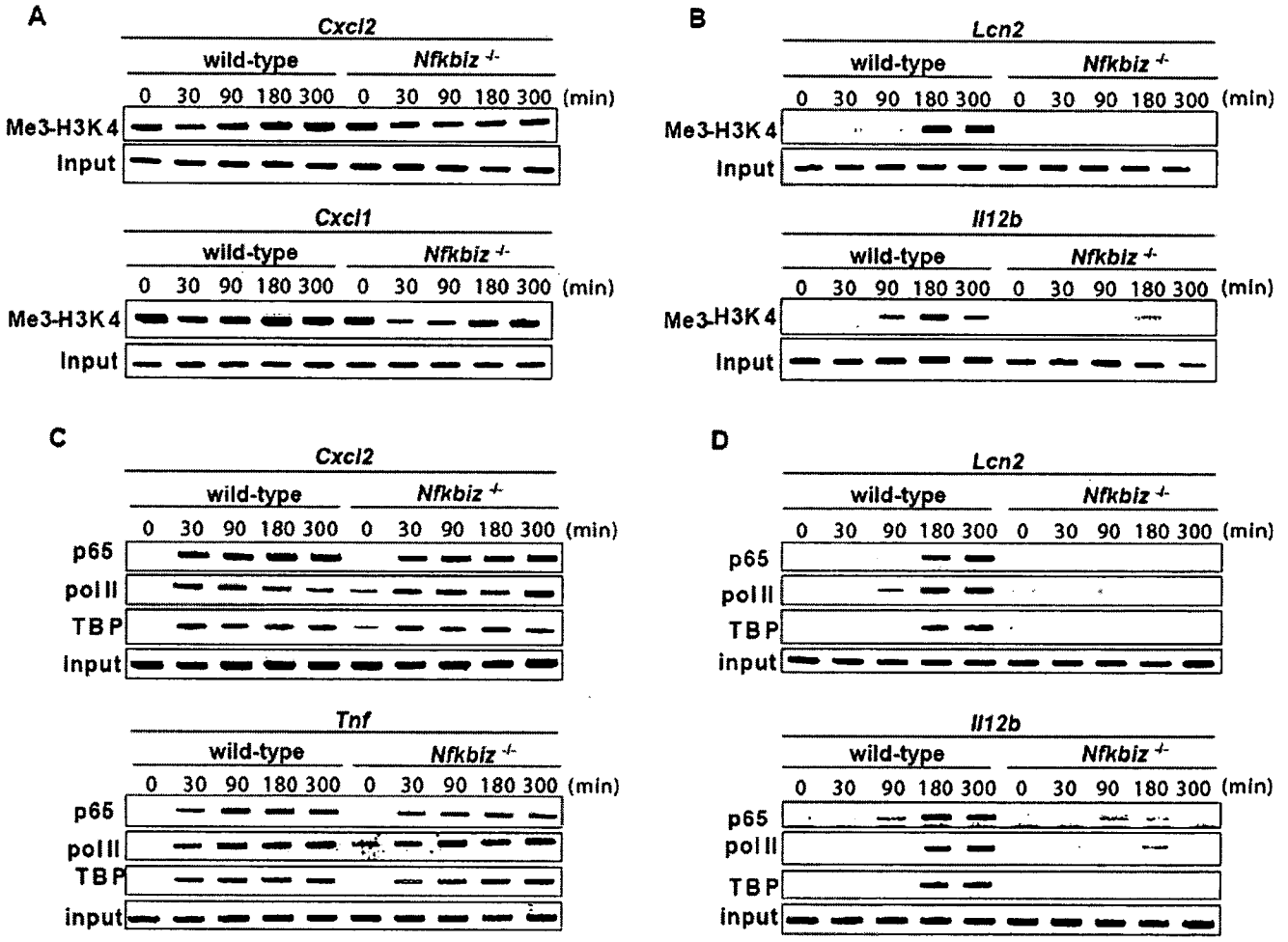
A
Cxcl2
wild-type
Nfkbiz -/-
0 30 90 180 300 0 30 90 180 300 (min)
Me3-H3K4
Input
Cxcl1
wild-type
Nfkbiz -/-
0 30 90 180 300 0 30 90 180 300 (min)
Me3-H3K4
Input
B
Lcn2
wild-type
Nfkbiz -/-
0 30 90 180 300 0 30 90 180 300 (min)
Me3-H3K4
Input
Il12b
wild-type
Nfkbiz -/-
0 30 90 180 300 0 30 90 180 300 (min)
Me3-H3K4
Input
C
Cxcl2
wild-type
Nfkbiz -/-
0 30 90 180 300 0 30 90 180 300 (min)
p65
polII
TBP
Input
Tnf
wild-type
Nfkbiz -/-
0 30 90 180 300 0 30 90 180 300 (min)
p65
polII
TBP
input
D
Lcn2
wild-type
Nfkbiz -/-
0 30 90 180 300 0 30 90 180 300 (min)
p65
polII
TBP
input
Il12b
wild-type
Nfkbiz -/-
0 30 90 180 300 0 30 90 180 300 (min)
p65
polII
TBP
input

Figure 5

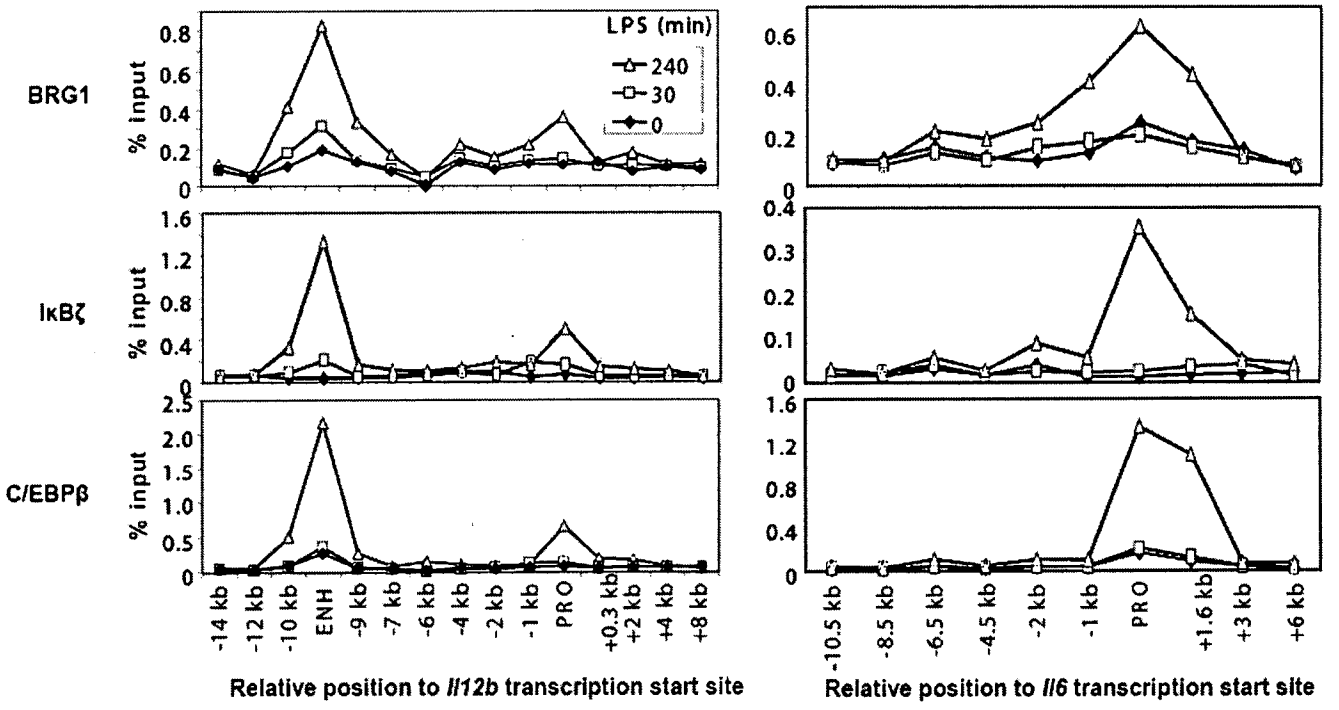
BRG1
IκBζ
C/EBPβ
% input
LPS (min)
240
30
0
-14 kb
-12 kb
-10 kb
ENH
-9 kb
-7 kb
-6 kb
-4 kb
-2 kb
-1 kb
PRO
+0.3 kb
+2 kb
+4 kb
+8 kb
-10.5 kb
-8.5 kb
-6.5 kb
-4.5 kb
-2 kb
-1 kb
PRO
+1.6 kb
+3 kb
+6 kb
Relative position to Il12b transcription start site
Relative position to Il6 transcription start site

Figure 6

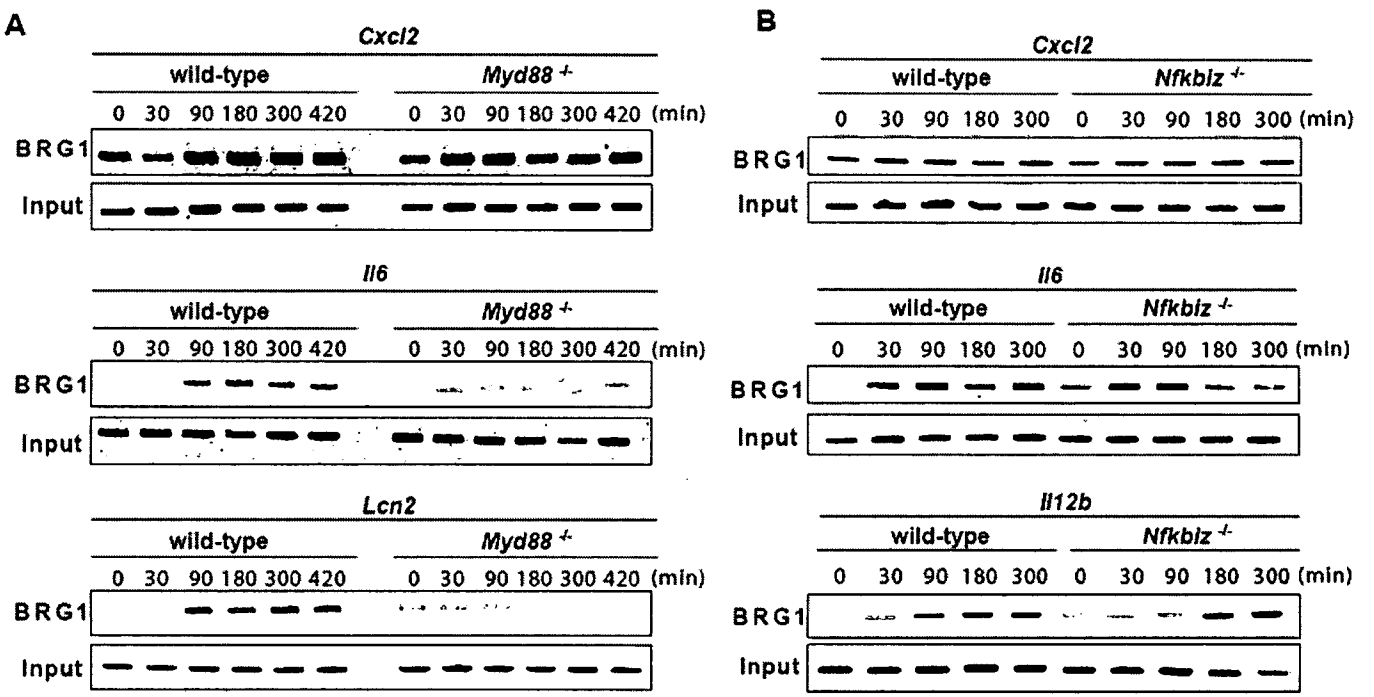
A
Cxcl2
wild-type
Myd88 -/-
0 30 90 180 300 420 0 30 90 180 300 420 (min)
BRG1
Input
Il6
wild-type
Myd88 -/-
0 30 90 180 300 420 0 30 90 180 300 420 (min)
BRG1
Input
Lcn2
wild-type
Myd88 -/-
0 30 90 180 300 420 0 30 90 180 300 420 (min)
BRG1
Input
B
Cxcl2
wild-type
Nfkbiz -/-
0 30 90 180 300 0 30 90 180 300 (min)
BRG1
Input
Il6
wild-type
Nfkbiz -/-
0 30 90 180 300 0 30 90 180 300 (min)
BRG1
Input
Il12b
wild-type
Nfkbiz -/-
0 30 90 180 300 0 30 90 180 300 (min)
BRG1
Input

Figure 7

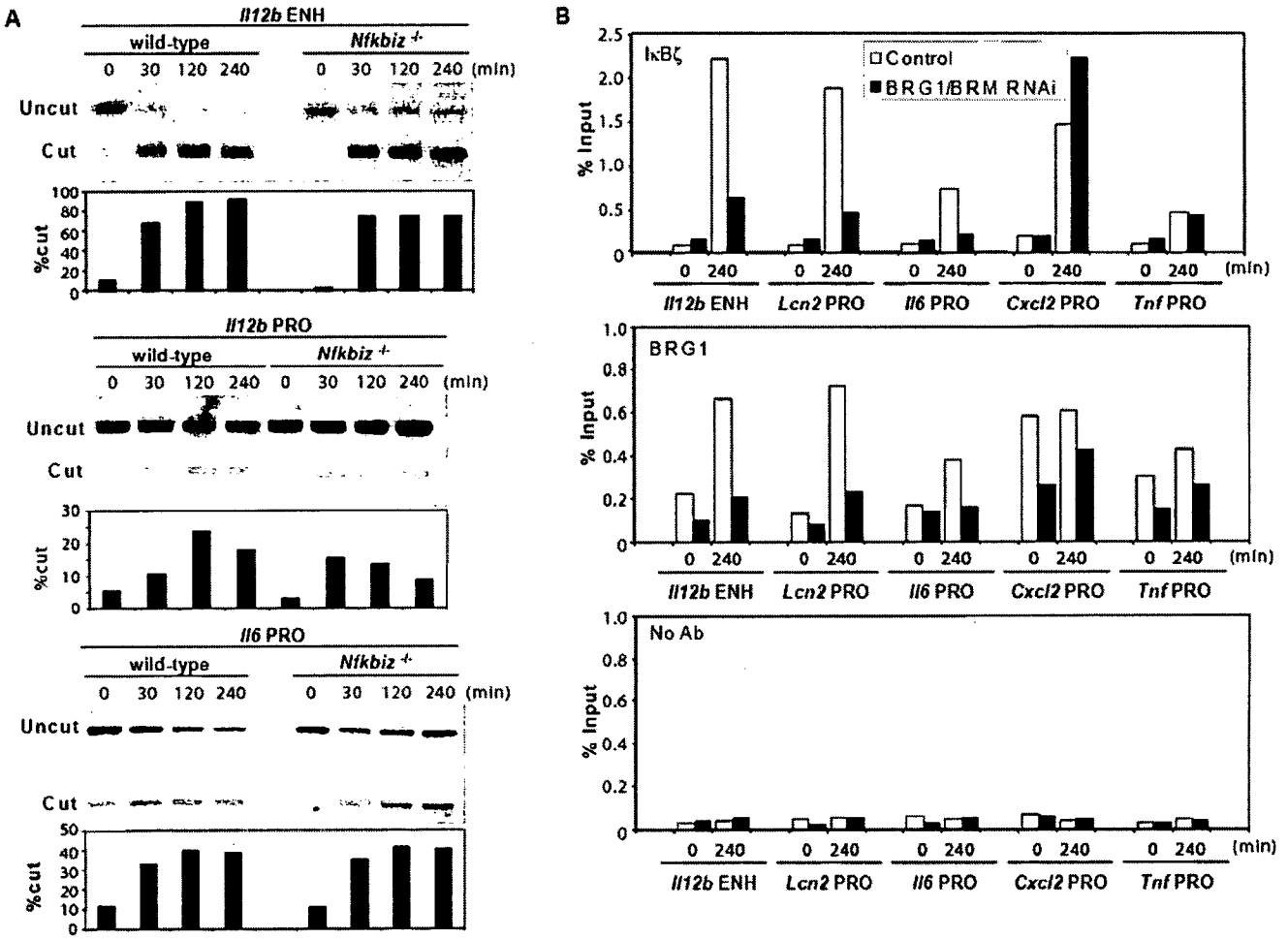
A
Il12b ENH
wild-type
Nfkbiz -/-
0 30 120 240 0 30 120 240 (min)
Uncut
Cut
%cut
Il12b PRO
Il6 PRO
B
IκBζ
Control
BRG1/BRM RNAi
% Input
BRG1
No Ab
0 240
(min)
Il12b ENH
Lcn2 PRO
Il6 PRO
Cxcl2 PRO
Tnf PRO

Figure 8

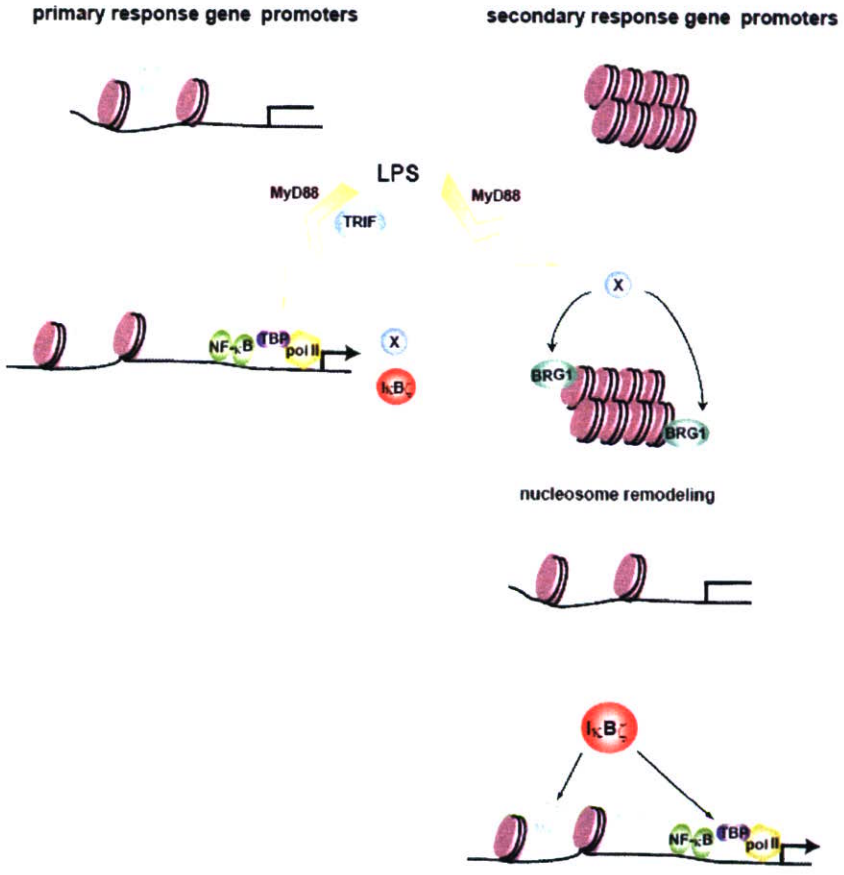
primary response gene promoters
secondary response gene promoters
LPS
MyD88
TRIF
MyD88
X
NF-κB
TBP
pol II
X
IκBζ
BRG1
BRG1
nucleosome remodeling
IκBζ
NF-κB
TBP
pol II

The Journal of Biological Chemistry

Supplementary Figure S1

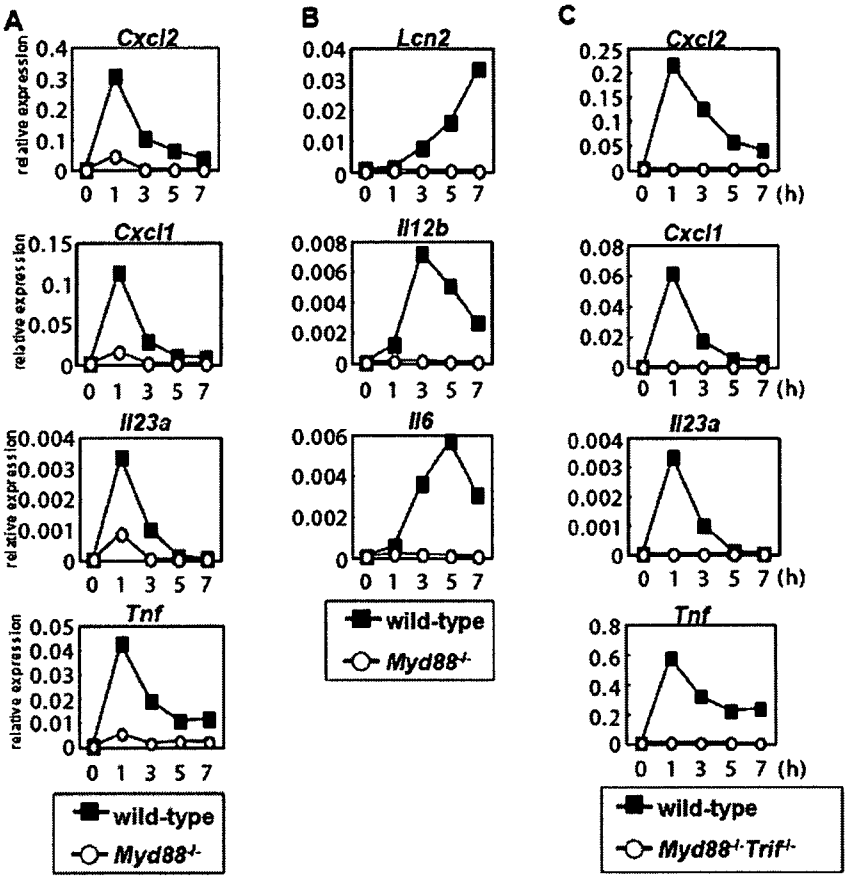

Supplementary figure S1 (A,B) Peritoneal macrophages from wild-type and *MyD88*$^{-/-}$ mice were stimulated with 100 ng/ml LPS for the indicated periods. Total RNA was extracted, and used for real-time RT-PCR analysis using primers specific for *Cxcl2, Cxcl1, Tnf, IL23a*(A), *Lcn2, IL12b* or *IL6* (B). The fold differences of each sample relative to EF-1α (Cxcl1, Tnf, IL12b, and IL6) or 18S rRNA (Cxcl2, IL23a, and Lcn2) levels are shown. Representative of at least two independent experiments. (C) Peritoneal macrophages from wild-type and *MyD88*$^{-/-}$ *TRIF*$^{-/-}$ mice were stimulated with 100 ng/ml LPS for the indicated periods. Total RNA was extracted,and used for real-time RT-PCR analysis as indicated in (A). Representative of at least two independent experiments.

The Journal of Biological Chemistry

Supplementary Figure S2

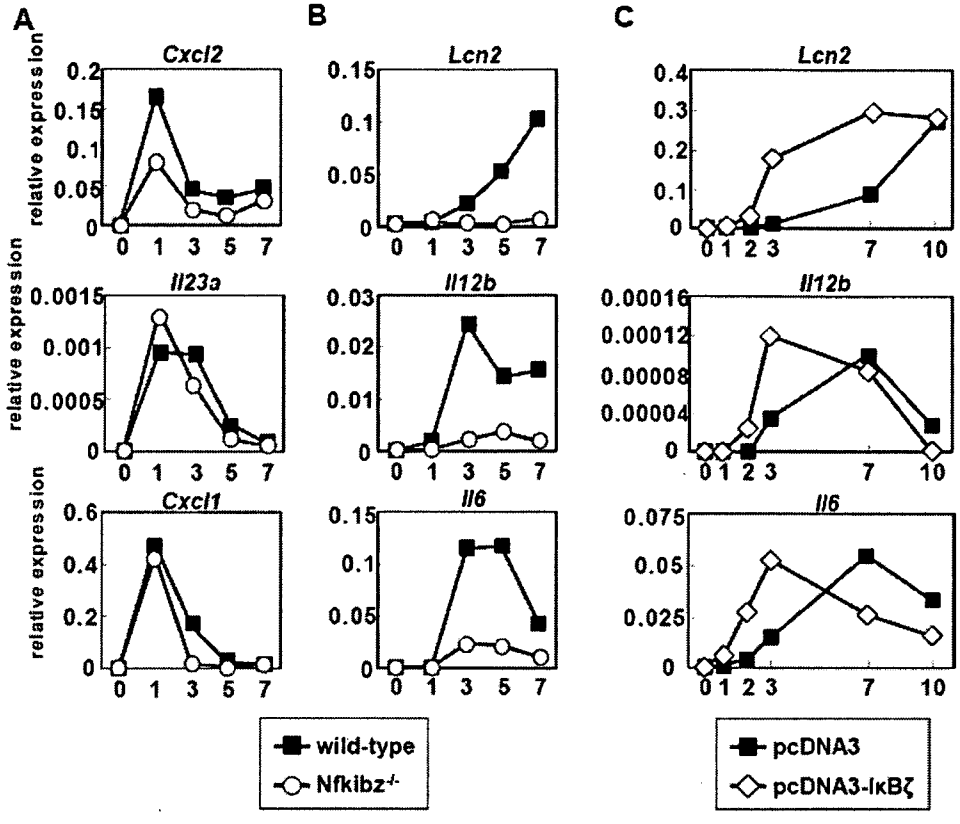

Supplementary figure S2 (A,B) Peritoneal macrophages from wild-type and *Nfkbiz*$^{-/-}$ mice were stimulated with 100 ng/ml LPS for the indicated periods. Total RNA was extracted, and used for real-time RT-PCR analysis using primers specific for *Cxcl2, IL23a, Cxcl1* (A), *Lcn2, IL12b* or *IL6* (B). The fold differences of each sample relative to EF-1α (*Cxcl1, IL12b, and IL6*) or 18S rRNA (*Cxcl2, IL23a, and Lcn2*) levels are shown. Representative of at least two independent experiments. (C) RAW cells were transfected with either control (pcDNA3) or IκBζ (pcDNA3-Ikbζ) expression plasmid. Stable transfectants were stimulated with 100 ng/ml LPS for the indicated periods. Total RNA was extracted, and used for real-time RT-PCR analysis using primers specific for *Lcn2, IL12b* and *IL6*. The fold differences of each sample relative to EF-1α (*IL12b* and *IL6*) or 18S rRNA (*Lcn2*) levels are shown.

Supplementary Figure S3

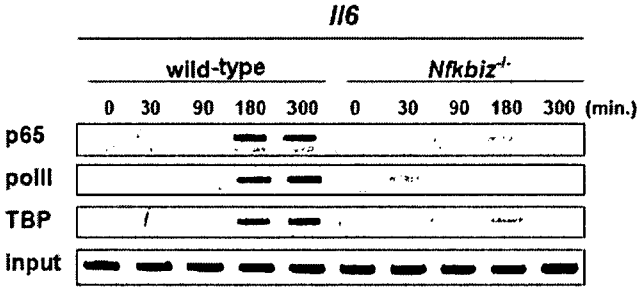

Supplementary Figure S3 Peritoneal macrophages from wild-type and *Nfkbiz*$^{-/-}$ mice were stimulated with 100 ng/ml LPS for the indicated periods, then chromatins were prepared and immunoprecipitated with antibody against NF-κBp65, pol II, or TBP. Precipitated DNA was analyzed by PCR with *Il6* promoter -specific primers.

The Journal of Biological Chemistry

Supplementary Figure S4

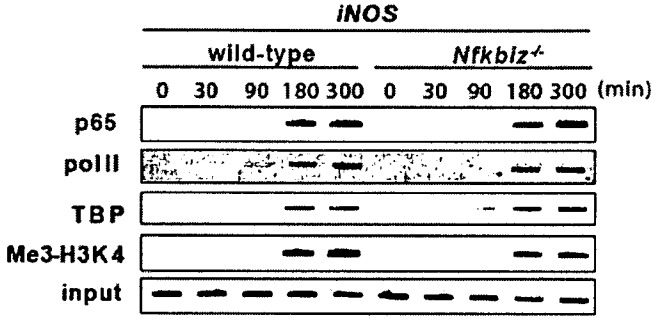

Supplementary figure S4 Chromatin prepared from wild-type and *Nfkbiz*$^{-/-}$ bone marrow-derived macrophages or peritoneal macrophages treated with 100 ng/ml LPS for the indicated periods was immunoprecipitated with antibodies against NF-κBp65, polII, TBP or trimethyl-histone H3 (Lys4). Precipitated DNA was analyzed by PCR with *iNOS* promoter specific primers.

Deoxynucleic Acids from *Cryptococcus neoformans* Activate Myeloid Dendritic Cells via a TLR9-Dependent Pathway[1]

Kiwamu Nakamura,[2*¶] Akiko Miyazato,[2*] Gang Xiao,[3†] Masumitsu Hatta,[*] Ken Inden,[*] Tetsuji Aoyagi,[*] Kohei Shiratori,[†] Kiyoshi Takeda,[‖] Shizuo Akira,[#] Shinobu Saijo,[**] Yoichiro Iwakura,[**] Yoshiyuki Adachi,[††] Naohito Ohno,[††] Kazuo Suzuki,[‡‡] Jiro Fujita,[¶] Mitsuo Kaku,[*‡§] and Kazuyoshi Kawakami[4†§]

The mechanism of host cell recognition of *Cryptococcus neoformans*, an opportunistic fungal pathogen in immunocompromised patients, remains poorly understood. In the present study, we asked whether the DNA of this yeast activates mouse bone marrow-derived myeloid dendritic cells (BM-DCs). BM-DCs released IL-12p40 and expressed CD40 upon stimulation with cryptococcal DNA, and the response was abolished by treatment with DNase, but not with RNase. IL-12p40 production and CD40 expression were attenuated by chloroquine, bafilomycin A, and inhibitory oligodeoxynucleotides (ODN) that suppressed the responses caused by CpG-ODN. Activation of BM-DCs by cryptococcal DNA was almost completely abrogated in TLR9 gene-disrupted (TLR9$^{-/-}$) mice and MyD88$^{-/-}$ mice, similar to that by CpG-ODN. In addition, upon stimulation with whole yeast cells of acapsular *C. neoformans*, TLR9$^{-/-}$ BM-DCs produced a lower amount of IL-12p40 than those from wild-type mice, and TLR9$^{-/-}$ mice were more susceptible to pulmonary infection with this fungal pathogen than wild-type mice, as shown by increased number of live colonies in lungs. Treatment of cryptococcal DNA with methylase resulted in reduced IL-12p40 synthesis by BM-DCs. Furthermore, using a luciferase reporter assay, cryptococcal DNA activated NF-κB in HEK293 cells transfected with the TLR9 gene. Finally, confocal microscopy showed colocalization of fluorescence-labeled cryptococcal DNA with CpG-ODN and the findings merged in part with the distribution of TLR9 in BM-DCs. Our results demonstrate that cryptococcal DNA causes activation of BM-DCs in a TLR9-dependent manner and suggest that the CpG motif-containing DNA may contribute to the development of inflammatory responses after infection with *C. neoformans*. *The Journal of Immunology*, 2008, 180: 4067–4074.

Cryptococcus neoformans (Cn)[5] is an opportunistic fungal pathogen and frequently causes fatal meningoencephalitis in patients with impaired immune responses, such as AIDS. It is an intracellular microorganism known to grow in macrophages, and has certain escape mechanisms that avoid killing by these cells (1). The host defense against Cn is largely mediated by cellular immunity (2) and CD4$^+$ T cells play a critical role in eradicating the infection (3, 4). The fate of this infection is greatly influenced by the Th1-Th2 cytokine balance: polarized Th1 immune response leads to protection, while biased synthesis of Th2 cytokines renders hosts prone to infection (5). Such balance is critically regulated by a variety of immune cells at an early stage after invasion of Cn into lung tissues, which includes dendritic cells (DCs), macrophages, NK cells, NKT cells, γδ T cells, and even neutrophils (6–10).

Invasion of microbial pathogens into tissues results in the development of inflammatory responses, which are initiated by recognition of pathogen-associated molecular patterns via pattern recognition receptors, such as TLRs (11). Using mice genetically lacking MyD88 or TLR2 (MyD88$^{-/-}$ or TLR2$^{-/-}$ mice), it was revealed that MyD88 plays a critical role while TLR2 plays a relatively limited role in the response to Cn (12). In another study (13), TLR2$^{-/-}$ mice as well as MyD88$^{-/-}$ mice succumbed to the infection, which was associated with reduced production of TNF-α, IL-2, and IFN-γ. In contrast, in our study (14), TLR2 and TLR4 did not seem to be involved in the host-protective response to this infection. In contrast, TLR4 was reported to sense glucuronoxylomannan, a major component of the polysaccharide capsule of Cn, in Chinese hamster ovary cells (15). Thus, the role of

*Department of Infection Control and Laboratory Diagnostics, Internal Medicine, Tohoku University Graduate School of Medicine, †Microbiology and Immunology, Department of Medical Technology, Tohoku University School of Health Sciences, ‡Comprehensive Research and Education Center for Planning of Drug Development and Clinical Evaluation Project, Tohoku University, and §Infection-Control Research Center, Tohoku University Hospital, Sendai; ¶Department of Medicine and Therapeutics, Control and Prevention of Infectious Diseases, Faculty of Medicine, University of the Ryukyus, Nishihara; ‖Department of Microbiology and Immunology, Graduate School of Medicine and #Department of Host Defense, Research Institute for Microbial Disease, Osaka University, Osaka; **Department of Microbiology and Immunology, Center for Experimental Medicine, Institute of Medical Science, University of Tokyo; ††Laboratory for Immunopharmacology of Microbial Products, Tokyo University of Pharmacy and Life Science, Tokyo; and ‡‡Department of Immunology, Inflammatory Program, Chiba University School of Medicine, Chiba, Japan

Received for publication July 20, 2007. Accepted for publication January 17, 2008.

The costs of publication of this article were defrayed in part by the payment of page charges. This article must therefore be hereby marked *advertisement* in accordance with 18 U.S.C. Section 1734 solely to indicate this fact.

[1] This work was supported by a Grant-in-Aid for Science Research (C) (18590413) from the Ministry of Education, Culture, Sports, Science and Technology of Japan, the Ministry of Health and Welfare of Japan, and Tohoku University 21st Center of Excellence Program "Comprehensive Research and Education Center for Planning of Drug Development and Clinical Evaluation Project."

[2] K.N. and A.M. contributed equally to this work.

[3] Current address: Department of Laboratory Medicine, The 6th Affiliated Hospital, Sun Yat-sen University School of Medicine, Guangzhou, China.

[4] Address correspondence and reprint requests to Dr. Kazuyoshi Kawakami, Microbiology and Immunology, Department of Medical Technology, Tohoku University School of Health Sciences, 2-1 Seiryo-cho, Aoba-ku, Sendai, Miyagi 980-8575, Japan. E-mail address: kawakami@mail.tains.tohoku.ac.jp

[5] Abbreviations used in this paper: Cn, *Cryptococcus neoformans*; DC, dendritic cell; BM-DC, bone marrow-derived DC; ODN, oligodeoxynucleotide; WT, wild type; OX-CA, NaClO-oxidized *Candida albicans*.

TLR2 and TLR4 in recognition of Cn remains to be fully understood, and some other TLR may be involved when considered along with the previous findings that the host-protective response was impaired in MyD88$^{-/-}$ mice (12, 13).

The unmethylated CpG motif-containing DNA from prokaryotic microorganisms such as bacteria and viruses is known to trigger host immune responses by interacting with TLR9 (16–18), which is distributed in the endosomal compartments (19, 20). Such interaction causes activation of signaling pathways mediated by an adaptor molecule, MyD88, leading to the synthesis of proinflammatory cytokines and expression of costimulatory molecules by macrophages and DCs (20, 21). In previous studies (22, 23), DNA from protozoa was reported to stimulate B cell proliferation and macrophage cytokine synthesis in a TLR9-dependent manner, although they are eukaryotic microorganisms. These findings raise a possibility that DNA from Cn may be involved in the activation of host immune responses, as in the case of protozoa. In agreement with this hypothesis, DNA from some fungi, such as *Schizosaccharomyces pompe* and *Paracoccidioides brasiliensis*, is also reported to stimulate a battery of immune responses (24, 25).

The main hypothesis of the present study was that DNA from Cn can induce the activation of DCs. The results showed that cryptococcal DNA stimulated bone marrow-derived DCs (BM-DCs) to synthesize cytokines and to express costimulatory molecules. These actions were completely dependent on the expression of TLR9. Furthermore, cryptococcal DNA was taken into the endosomal compartment in a manner similar to the synthetic CpG-oligodeoxynucleotide (ODN) and triggered a signaling pathway for the activation of NF-κB via TLR9.

Materials and Methods

Mice

TLR9$^{-/-}$, MyD88$^{-/-}$, Dectin-1$^{-/-}$, and TRIF$^{-/-}$ mice were generated, as described previously (18, 26–28). Homozygous mice were backcrossed to C57BL/6 mice for more than eight generations. Male or female mice at 6–10 wk of age were used for the experiments and wild-type (WT) C57BL/6 mice were used as controls. All of the mutant mice were kept under specific pathogen-free conditions at Oriental Biosciences (Kyoto, Japan), the Center for Experimental Medicine, Institute of Medical Science, University of Tokyo, and Kyusyu University, respectively. The experiments were conducted according to the institutional guidelines and were approved by the institutional ethics committees.

Microorganisms

The acapsular strain of Cn, designated as Cap67 (a gift from Dr. S. M. Levitz, Boston University, Boston, MA) and its parent strain, designated as B3501 (a gift from Dr. K. Chung, National Institutes of Health, Bethesda, MD) were used. Serotype A-encapsulated strains of Cn, designated as YC-11 and 13, were established from patients with pulmonary cryptococcosis (29). The yeast cells were cultured on potato dextrose agar plates (Eiken) for 2–3 days before use.

Pulmonary infection and enumeration of viable Cn

To induce pulmonary infection, mice were anesthetized by i.p. injection of 70 mg/kg pentobarbital (Abbott Laboratories) and restrained on a small board. Live Cn, Cap67 strain (5×10^6 cells), were inoculated at 50 μl/mouse by insertion of a 25-gauge blunt needle into and parallel to the trachea. Mice were sacrificed 2 wk after infection, and lungs and brains were dissected carefully and excised, then separately homogenized in 5 and 2 ml of distilled water, respectively, by teasing with a stainless mesh at room temperature. The homogenates, appropriately diluted with distilled water, were inoculated at 100 μl on potato dextrose agar plates, cultured for 2–3 days, followed by counting the number of colonies.

Preparation of Cn lysates and DNA

Cn yeast cells (1×10^{11}) were treated with 70% ethanol for 30 min, washed three times with PBS, and then received five cycles of disruption with 0.3 mm of zirconia beads by use of Multibeads shocker (Yasui Kikai). For preparation of Cn DNA, the yeast cells were lysed with 100 mM Tris-hydrochloride (pH 7.5), 0.5% SDS, and 30 mM EDTA at 100°C for 15 min. The DNA was purified by extraction with phenol/chloroform/isoamyl alcohol (25:24:1) and isopropanol precipitation. The pellet was washed with 70% ethanol, dried, and resolved with distilled water. The obtained DNA was kept at −20°C until use. The OD_{260}:OD_{280} ratio was usually between 1.5 and 2.0. The endotoxin content in the DNA preparations measured by *Limulus* amebocyte lysate assay was <10 pg/ml.

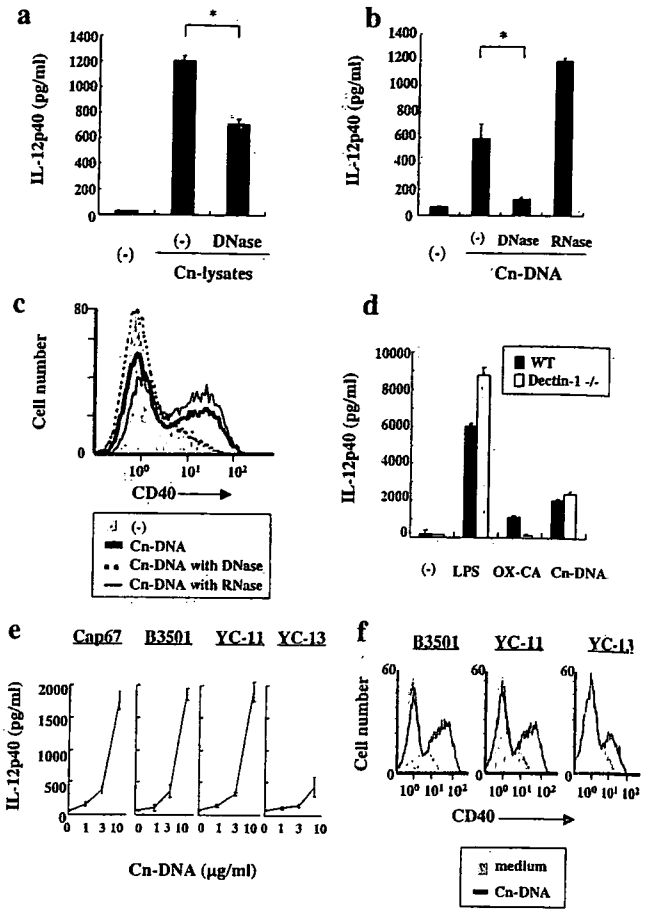

FIGURE 1. DNA from Cn activate BM-DCs. BM-DCs were cultured with various stimulants for 24 h. IL-12p40 levels were assayed by ELISA and surface expression of CD40 on BM-DCs was determined by flow cytometry. *a*, BM-DCs were cultured with 1% Cap67 lysates that were pretreated or not with DNase. *b* and *c*, BM-DCs were cultured with 10 μg/ml Cap67 DNA pretreated or not with DNase or RNase. *d*, BM-DCs from dectin-1$^{-/-}$ or WT mice were cultured with LPS (1 μg/ml), OX-CA (1 μg/ml), or Cap67 DNA (10 μg/ml). *e* and *f*, BM-DCs were cultured with DNA from Cap67, B3501, YC-11, and YC-13 at the indicated doses. Data are the mean ± SD of triplicate cultures. Flow cytometry data are representative of three independent experiments. *, $p < 0.05$.

Culture medium and reagents

RPMI 1640 medium was obtained from Nippro and FCS from Cansera. Bafilomycin A, DNase, RNase, peptidoglycan (PG), and LPS were purchased from Sigma-Aldrich, polymixin B from MP Bioscience, and chloroquine from Wako Biochemicals. NaClO-oxidized *Candida albicans* (OX-CA: a particle form β-1,6-branched β-1,3-glucan was prepared as described previously (30)). CpG-ODN (CpG1826: TCC ATG ACG TTC CTG ACG TT) and inhibitory ODN (ODN2088 and 2114), TCC TGG CGG GGA AGT and TCC TGG ACG GGA AGT, respectively, were synthesized at Hokkaido System Science. All ODN were phosphorothioated and purified by HPLC. The endotoxin content measured by *Limulus* amebocyte lysate assay was <10 pg/ml.

Preparation of Cn culture supernatants

Cn yeast cells (YC-11) were cultured at 1×10^6/ml in RPMI 1640 medium supplemented with 10% FCS, 100 U/ml penicillin G, and 100 μg/ml streptomycin for 48–72 h in a 5% CO_2 incubator. The culture supernatants were

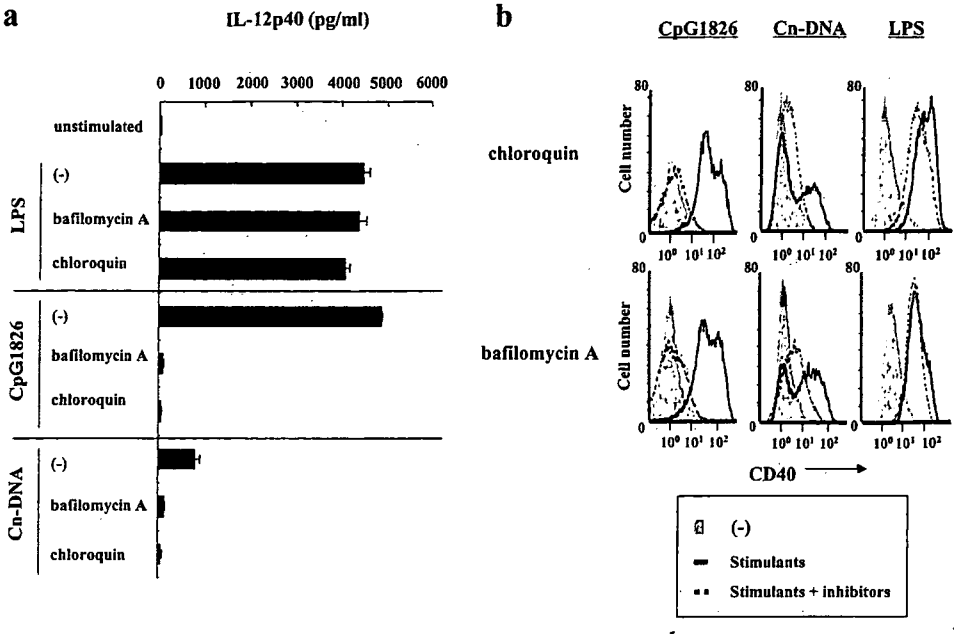

FIGURE 2. Effects of chloroquine and bafilomycin A. BM-DCs pretreated or not with chloroquine (3 μg/ml) or bafilomycin A (60 nM) were cultured with LPS (1 μg/ml), CpG1826 (150 nM), or Cap67 DNA (10 μg/ml). IL-12p40 levels in the culture supernatants (*a*) and expression of CD40 on BM-DCs (*b*) were measured. Data are mean ± SD of triplicate cultures. Flow cytometry data are representative of three independent experiments.

collected and passed through 0.2-μm Millipore filter and kept at −70°C before use.

Treatment of DNA with DNase, RNase, and methylase

Cap67 DNA was incubated with 10 μg/ml DNase or RNase in water bath at 37°C for 4 h. After incubation, the DNAs were heated at 68°C for 20 min to inactivate DNase and again purified by isopropanol precipitation. Methylated dsCpG1826 or Cap67 DNA was synthesized by incubating each DNA with Sss CpG methylase (10 U/μg DNA) for 24 h at 37°C in a water bath. Then, DNAs were heated at 68°C for 20 min to inactivate Sss CpG methylase and centrifuged by adding isopropanol for purification.

Preparation and culture of DCs

DC were prepared from BM cells as described by Lutz et al. (31), with some modifications. Briefly, BM cells from WT, TLR9KO, MyD88KO, TRIFKO, and dectin-1KO mice were cultured at 2×10^5/ml in 10 ml RPMI 1640 medium supplemented with 10% FCS (Cansera), 100 U/ml penicillin G, 100 μg/ml streptomycin, and 50 μM 2-ME containing 20 ng/ml murine GM-CSF (WakoCytomation). On day 3, 10 ml of the same medium was added, followed by a half change with the GM-CSF-containing culture medium on day 6. On day 8, nonadherent cells were collected and used as BM-DCs. The obtained cells were cultured at 1×10^5/ml with various stimulants for 24 h at 37°C in 5% CO_2 incubator.

Cytokine assay

The concentration of IL-12p40 in the culture supernatants was measured by ELISA using capture and biotinylated developing Abs (BD Biosciences). The detection limit was 15 pg/ml.

Flow cytometric analysis

Cells were preincubated with anti-FcγRII and III mAb, prepared by a protein G column kit (Kirkegaard & Perry Laboratories) from the culture supernatants of hybridoma cells (clone 2.4G2), on ice for 15 min in PBS containing 1% FCS and 0.1% sodium azide, stained with FITC-conjugated anti-CD11c mAb (clone HL3; BD Biosciences), and PE-conjugated anti-CD40 mAb (clone 1C10; eBioscience) for 25 min and then washed three times in the same buffer. Isotype-matched irrelevant Abs were used for control staining. The propidium iodide-stained population was excluded as dead cells. The stained cells were analyzed using a Cytomics FC500 flow cytometer (Beckman Coulter). Data were collected from 15,000 to 20,000 individual live cells using parameters of forward scatter/side scatter and FL1 to set a gate on the $CD11c^+$ lymphocyte population.

TLR9 cloning and NF-κB reporter assay

The full-length *tlr9* was PCR amplified from a cDNA of mouse macrophage cell line RAW264.7 cells (RIKEN Cell Bank). Specific primers for amplification of *tlr9* were designed based on the GenBank accession number AF314224 (32). The sequences of primers were 5′-CAC CAT GGT TCT CCG TCG AAG G-3′ (forward) and 5′-CTA TTC TGC TGT AGG TCC CCG GC-3′ (reverse). The amplified full-length cDNA was cloned

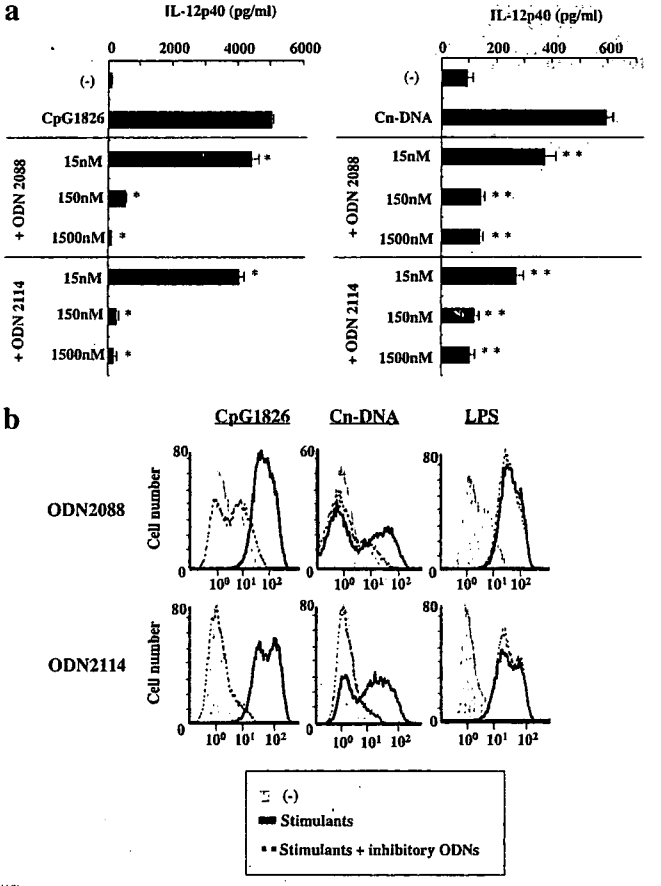

FIGURE 3. Effect of inhibitory ODN. BM-DCs were cultured with CpG1826 (150 nM) or Cap67 DNA (10 μg/ml) in the presence or absence of the indicated doses of ODN2088 or ODN2114. IL-12p40 levels in the culture supernatants (*a*) and expression of CD40 on BM-DCs (*b*) were measured. Data are mean ± SD of triplicate cultures. * and **, $p < 0.05$, compared with CpG1826 and Cn-DNA, respectively. Flow cytometry data are representative of three independent experiments.

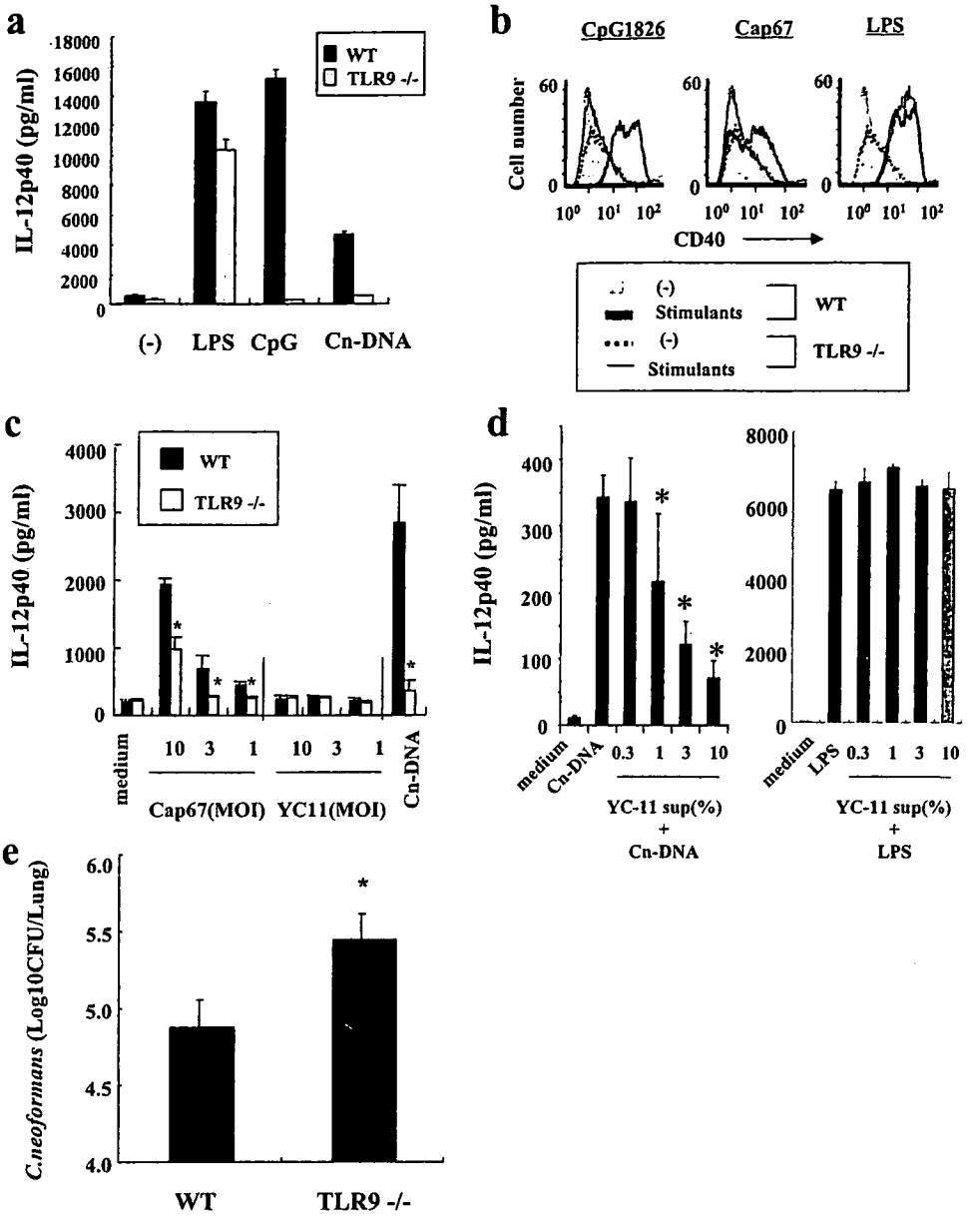

FIGURE 4. Cryptococcal DNA require TLR9 for activation of BM-DCs. BM-DCs from TLR9$^{-/-}$ or WT mice were cultured with LPS (1 μg/ml), CpG1826 (150 nM), or Cap67 DNA (10 μg/ml). IL-12p40 levels in the culture supernatants (*a*) and expression of CD40 on BM-DCs (*b*) were measured. Data are mean ± SD of triplicate cultures. Flow cytometry data are representative of two independent experiments. *c*, BM-DCs from TLR9$^{-/-}$ or WT mice were cultured with the indicated doses of Cap67 or YC-11 for 24 h, in which the extracellular yeast cells were not washed away. IL-12p40 levels in the culture supernatants were measured. Data are mean ± SD of triplicate cultures. MOI, Multiplicity of infection. *, $p < 0.05$, compared with WT mice. *d*, BM-DCs from WT mice were cultured with Cap67 DNA (10 μg/ml) or LPS (1 μg/ml) in the presence or absence of the indicated doses of YC-11 culture supernatants for 24 h, and the concentrations of IL-12p40 in the culture supernatants were measured. Data are mean ± SD of triplicate cultures. sup, Culture supernatants. *, $p < 0.05$, compared with the cultures without YC-11 culture supernatants. *e*, TLR9$^{-/-}$ or WT mice were infected intratracheally with Cap67 (5×10^6/mouse) and the number of live colonies in lungs was counted on day 14 after infection. Data are mean ± SD of seven mice. *, $p < 0.05$, compared with WT mice.

into pcDNA6.2/TOPO (Invitrogen Life Technologies) and sequenced. Endothelial leukocyte adhesion molecule 1 luciferase reporter plasmids were provided by Dr. M. Mitsuyama (Kyoto University, Kyoto, Japan). For the NF-κB luciferase reporter assay, HEK293T cells were transiently transfected with 100 ng of reporter plasmid along with 100 ng of *tlr9* expression plasmids or empty control plasmid. At 24 h after transfection, the cells were treated with PG, CpG-ODN, or cryptococcal DNA for 6 h. Luciferase activity in the total cell lysate was measured with the dual-luciferase reporter assay system (Promega). The *Renilla*-luciferase reporter gene was simultaneously transfected as an internal control. Relative luciferase activities were calculated as folds of induction compared with unstimulated vector control.

Florescent labeling and confocal imaging Cap67

DNA was labeled with Alexa Fluor 647 using ULYSIS Nucleic Acid Labeling kits (Molecular Probes) according to the instructions provided by the manufacturer. The relative efficiency of a labeling reaction was evaluated by calculating the approximate ratio of bases to dye molecules. Rhodamine-labeled CpG-ODN was purchased from Hokkaido System Science. FITC-conjugated TLR9 mAb (clone 26C593.2) was purchased from IMGENEX. Cells were incubated in microtubes, cytospun to glass slides, and coverslips were mounted on the glass slides with a ProLong Antifade Kit (Molecular Probes). Confocal studies were performed with an oil immersion objective (×60 Plan Apo; numerical aperture 1.4) and a Nikon TIRF-C1 confocal microscope. The software, Nikon EZ-C1 version 2.00, were used to acquire and process the confocal images. Dual-color images were acquired using a sequential acquisition mode to avoid cross-excitation.

Statistical analysis

Analysis was conducted using Statview II software (Abacus Concept) on a Macintosh computer. Data are expressed as mean ± SD. Differences between groups were examined for statistical significance using one-way ANOVA with a post hoc analysis (Fisher (plausible least significant difference) PLSD test). A value of $p < 0.05$ was considered significant.

Results

DNA from Cn activates BM-DCs

We measured the activity of Cn to induce the synthesis of IL-12p40 by BM-DCs. For this purpose, we used the acapsular mutant strain Cap67 to avoid the influence of capsular polysaccharides, which were reported to suppress various immune responses (33). The lysates of Cap67 prepared using a multibeads shocker generated IL-12p40 by BM-DCs. We tested the effect of DNase on the cytokine-inducing capability of Cap67 lysates. As shown in Fig. 1*a*, DNase significantly reduced the production of both cytokines.

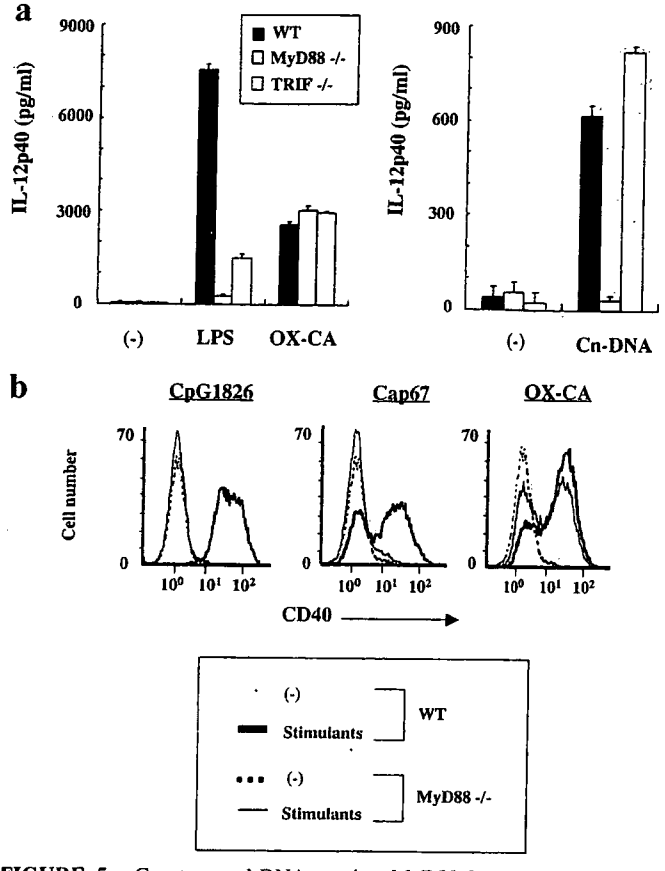

FIGURE 5. Cryptococcal DNA requires MyD88 for activation of BM-DCs. BM-DCs from MyD88$^{-/-}$, TRIF$^{-/-}$, or WT mice were cultured with LPS (1 μg/ml), OX-CA (1 μg/ml), or Cap67 DNA (10 μg/ml). *a*, IL-12p40 levels in the culture supernatants were measured. Data are mean ± SD of triplicate cultures. *b*, Flow cytometry data are representative of two independent experiments.

These results suggest the involvement of Cap67 DNA in this response. Next, we tested whether Cap67-derived DNA can activate BM-DCs by measuring the synthesis of IL-12p40 and expression of CD40 on these cells. IL-12p40 was produced by this stimulation in a dose-dependent manner and such production was completely abolished by the addition of DNase, but not of RNase (Fig. 1*b*). Similarly, the expression of CD40 on BM-DCs was accelerated by coculture with Cap67 DNA, and this effect was inhibited by DNase, but not by RNase (Fig. 1*c*). These responses were not affected by the addition of polymixin B, which completely abolished cytokine production induced by LPS (data not shown), indicating that the activity of Cap67 DNA was not mediated by LPS contamination. Since fungi secrete β-glucan that activates BM-DCs (34), it is possible that β-glucan contaminating the DNA preparation could have mediated these responses. However, this was not the case, because IL-12p40 produced by Cap67 DNA-stimulated BM-DCs was not decreased in mice lacking dectin-1, the sole receptor of β-glucan (Fig. 1*d*). Furthermore, we tested also whether these findings were specific for this particular mutant strain of Cn. IL-12p40 synthesis by BM-DCs was induced by DNA derived from the parent strain of Cap67, B3501, and two clinically isolated strains, YC-13 and YC-11, in a dose-dependent fashion (Fig. 1*e*). Similarly, the expression of CD40 on BM-DCs was enhanced by DNA from these strains (Fig. 1*f*). These results indicate that DNA from Cn directly activated BM-DCs to synthesize the cytokine and to express the surface activation Ag. In contrast, DNA derived from mouse splenocytes and human PBMC did not induce these responses by BM-DCs (data not shown).

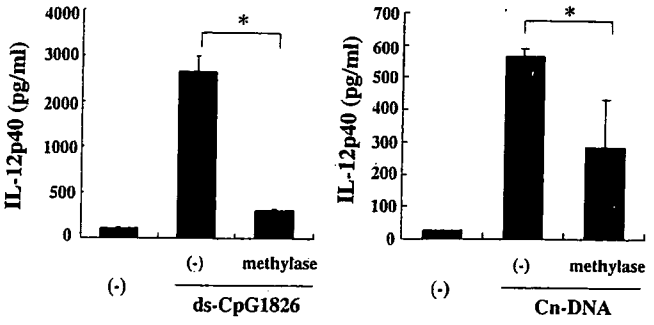

FIGURE 6. Effect of methylation of cryptococcal DNA. BM-DCs were cultured with dsCpG1826 (4.5 μM) or Cap67 DNA (10 μg/ml) pretreated or not with methylase. IL-12p40 levels in the culture supernatants were measured. Data are mean ± SD of triplicate cultures. *, $p < 0.05$.

DNA of Cn activates BM-DCs in a manner similar to CpG-ODN

Because Cn is a eukaryote, we questioned whether the activity of DNA from this fungal pathogen is different from that of a synthetic ODN containing the CpG motif, which prokaryote DNA usually carries in an unmethylated form (17). Previous studies reported that CpG-ODN-induced activation of BM-DCs was strongly inhibited by chloroquine and bafilomycin A, both of which interfere with endosomal maturation (35). Therefore, to address this issue, we compared the effects of these inhibitors on the synthesis of IL-12p40 by BM-DCs and expression of CD40 caused by a stimulatory CpG-ODN (CpG1826) and Cap67 DNA. As shown in Fig. 2*a*, the synthesis of IL-12p40 by Cap67 DNA-stimulated cells was strongly suppressed by addition of either chloroquine or bafilomycin A; such an effect was similar to the responses induced by CpG1826, but not by LPS. Similarly, the addition of chloroquine or bafilomycin A suppressed CD40 expression induced by Cap67 DNA and CpG1826, but not by LPS (Fig. 2*b*).

Previous studies identified DNA sequences that neutralized the CpG-ODN-induced activation of B cells (36). In the next experiments, therefore, we tested the effect of such ODN with an inhibitory DNA motif on the induction of IL-12p40 synthesis and CD40 expression by BM-DCs. As shown in Fig. 3, ODN2088 and ODN2114 strongly inhibited these responses induced by both CpG1826 and Cap67 DNA, whereas such inhibition was not detected on the responses by LPS. These results indicate that Cn DNA exerted its activity in a manner similar to CpG1826 and suggest that the fungal DNA may activate BM-DCs via interaction with TLR9, a recognition receptor of the unmethylated CpG motif (17, 18).

Cn DNA requires TLR9 for activation of BM-DCs

To address this possibility, we investigated the role of TLR9 in Cap67 DNA-induced BM-DC activation. As shown in Fig. 4, *a* and *b*, production of IL-12p40 and expression of CD40 by Cap67 DNA- and CpG1826-stimulated cells were completely diminished in TLR9$^{-/-}$ mice, whereas such effect was not detected when the cells were stimulated with LPS. In this study, it should be noted that DNA was not released from Cn outside the DCs, but rather likely generated from the killed yeast cells in the endosomal compartments. Therefore, our current observations indicating the activation of BM-DCs by cryptococcal DNA have a more physiological significance, when defective expression of TLR9 interferes with activation induced by whole Cn. As shown in Fig. 4*c*, the amount of IL-12p40 synthesized by BM-DCs in response to whole yeast cells of Cap67, an acapsular strain, was significantly reduced in TLR9$^{-/-}$ mice compared with WT control mice, whereas YC-11, a highly encapsulated strain, failed to induce the production of

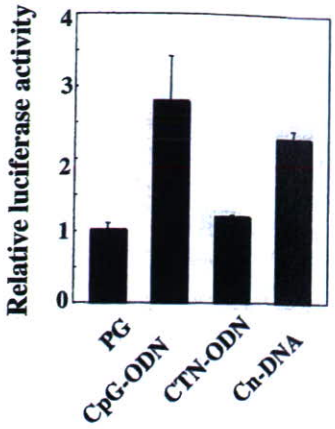

FIGURE 7. NF-κB activation via TLR9 by cryptococcal DNA. HEK293T cells transfected with the TLR9 gene or control vector were treated with CpG1826 (300 nM), PG (1 μg/ml), or Cap67 DNA (250 μg/ml) for 6 h. The luciferase activity in each sample was determined as described in *Materials and Methods*. Data are expressed as relative values to those of control vector and presented are mean ± SD of triplicate cultures. CNT-ODN, control ODN of CpG1826.

IL-12p40 by BM-DCs from both mice, which may raise a possibility that capsular polysaccharides affect the activation of BM-DCs caused by cryptococcal DNA. We tested the effect of the culture supernatants of YC-11 on the IL-12p40 production by BM-DCs. As shown in Fig. 4*d*, the production of this cytokine caused by cryptococcal DNA was strongly inhibited by the YC-11 culture supernatants in a dose-dependent fashion, whereas such inhibition was not found when BM-DCs were stimulated with LPS. In addition, we compared the clinical course of infection with Cap67 in lungs between TLR9$^{-/-}$ and WT mice. As shown in Fig. 4*e*, the number of live colonies in lungs was significantly higher in the former mice than in the latter ones 2 wk after infection, although dissemination of yeast cells to brains was not detected in both groups (data not shown).

In additional experiments, we tested how Cap67 DNA-induced activation of BM-DCs was affected in mice genetically lacking MyD88, a downstream signaling molecule of TLR9 and TLR4, or TRIF, that of TLR4, but not of TLR9 (37). BM-DCs from MyD88$^{-/-}$ mice failed to produce IL-12p40 induced by Cap67 DNA and LPS, but not by OX-CA (Fig. 5*a*). In contrast, LPS, but not Cap67 DNA and OX-CA, inhibited such production by BM-DCs from TRIF$^{-/-}$ mice (Fig. 5*a*). Similarly, CD40 expression induced by Cap67 DNA and CpG1826 was completely abrogated in MyD88$^{-/-}$ mice, whereas such expression was not affected in the case of OX-CA stimulation (Fig. 5*b*). Similar results were obtained for the synthesis of IL-12p40, when BM-DCs were stimulated with whole yeast cells (data not shown). These results indicate that TLR9 and its downstream signaling molecule are essential for Cap67 DNA-induced activation of BM-DCs.

Methylation of the CpG motif results in the loss of its capability to activate DCs via a TLR9-dependent signaling pathway (16, 24). Therefore, we tested the effect of methylation on cytokine synthesis by Cap67 DNA-stimulated BM-DCs. As shown in Fig. 6, BM-DCs stimulated by CpG1826 and Cap67 DNA pretreated with methylase did not synthesize IL-12p40. These results were consistent with the notion that Cn DNA activates BM-DCs by interacting with TLR9.

Cn DNA activates the signaling pathway via TLR9

CpG-ODN triggers the signaling pathway via TLR9, which results in the activation of NF-κB (37). In the next step, we tested the effect of Cn DNA on NF-κB. For this purpose, we performed a luciferase reporter assay using HEK293T cells transfected with the gene for TLR9 and luciferase gene linked to the promoter sequence containing an NF-κB binding site. As shown in Fig. 7, both Cap67 DNA and CpG1826 induced luciferase activity in TLR9-expressing HEK293T cells, whereas PG and control ODN of CpG1826 did not show such activity. These results indicate that Cn DNA triggered the signaling pathway for activation of NF-κB by directly interacting with TLR9.

Colocalization of Cn DNA with CpG-ODN in BM-DCs

In DCs and macrophages, CpG-ODN is internalized into early endosomes, followed by subsequent transportation to a lysosomal compartment and direct interaction with TLR9, which is redistributed from the endoplasmic reticulum (19, 20). Using confocal microscopic analysis, we compared the intracellular trafficking of Cap67 DNA and CpG1826 to further define the relationship of both agents during the activation of BM-DCs. As shown in Fig. 8*a*, Cap67 DNA and CpG1826 were mostly colocalized in the intracellular area of BM-DCs at 5, 30, 60, and 90 min after incubation. Thus, the intracellular trafficking of Cn DNA in BM-DCs is similar to that of CpG1826, suggesting the interaction of the fungal DNA with TLR9. In the next step, we analyzed the distribution of TLR9 in these cells after incubation with Cap67 DNA and CpG1826. Isotype-matched irrelevant Ab did not show positive staining in resting and Cap67 DNA-stimulated BM-DCs (data not shown). TLR9 was detected in the intracellular area of resting BM-DCs and redistributed in part to the area where these nucleic acids were localized after stimulation, and similar results were obtained using RAW264.1 cells, a macrophage lineage cell line (Fig. 8*b*). These results indicate that Cn DNA interacts with TLR9 in the endosomal pathway similar to CpG1826.

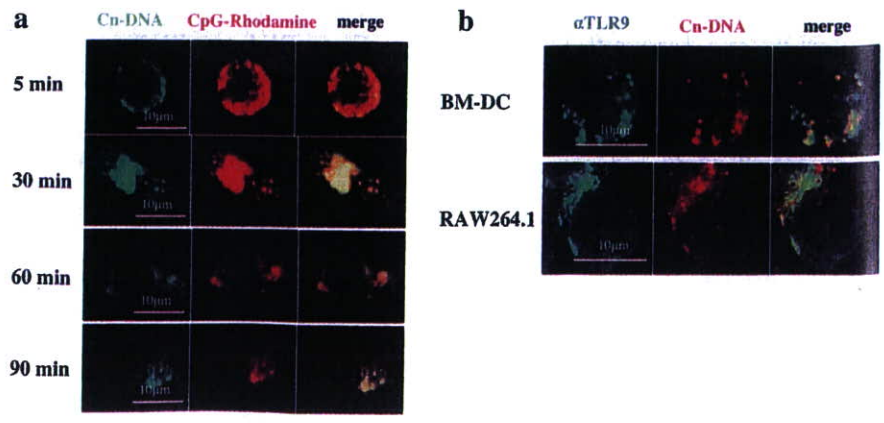

FIGURE 8. Trafficking of cryptococcal DNA in BM-DCs and colocalization with TLR9. *a*, BM-DCs were simultaneously incubated with 10 μg/ml Alexa Fluor 647-conjugated Cap67 DNA (green) and 3 μM CpG-rhodamine (red) for the indicated time periods. *b*, BM-DCs or RAW264.1 cells were incubated with 10 μg/ml Alexa Fluor 647-Cap67 DNA (red) for 30 min. After fixation, TLR9 was stained intracellularly by direct immunofluorescence with FITC-conjugated anti-TLR9 Ab (green). Cells were analyzed using a confocal microscope. Data are representative of three to four independent experiments.

Discussion

In the present study, we hypothesized that DNA from Cn can activate BM-DCs based on the finding that lysates of this fungal microorganism showed such activity, which was significantly reduced after DNase treatment. In agreement with this hypothesis, cryptococcal DNA induced the release of IL-12p40 and expression of CD40 by BM-DCs. Such activity was not mediated by contaminated LPS or β-glucan due to the following reasons: 1) the activity was abrogated by DNase treatment, 2) polymixin B did not affect the activity, and 3) the level of activity was similar in BM-DCs from control mice, C3H/HeJ, and TLR4$^{-/-}$ mice (data not shown) and from dectin-1$^{-/-}$ mice lacking a specific receptor for β-glucan. In addition, activation of BM-DCs did not involve capsular polysaccharides because DNA from an acapsular strain of Cn was highly active. In earlier studies (24, 25), similar to our findings, DNA from two yeast-form fungi, *S. pompe* and *P. brasiliensis*, also induced the B cell proliferation and the development of Th1 immune responses and host protection, respectively, although the precise mechanism was not investigated. Thus, Cn seems to possess immunostimulatory DNA that promotes Th1-mediated host responses against this infection.

In previous studies (12, 13), MyD88, which acts as an adaptor molecule in signaling via TLRs (37), was reported to play an important role in host defense against cryptococcal infection. These findings suggested the possible involvement of certain TLRs. However, involvement of TLR2 and TLR4 in the host defense responses against this infection remains to be substantiated (12–14). Recent studies have identified the involvement of TLRs in the recognition of nucleic acids; including TLR3 for dsRNA, TLR7/8 for ssRNA, and TLR9 for unmethylated CpG motif-containing DNA (18, 38–40). Thus, we addressed the possible contribution of TLR9 to the mechanism underlying cryptococcal DNA-induced BM-DC activation, although it was unclear whether Cn possess such motifs in its DNA structure. CpG-ODN is internalized via an endocytic pathway and trafficked into late endosomal compartments, followed by direct interaction with TLR9 (19, 20). In this process, acidification of the endosomal compartments is required, which is blocked by chloroquine and bafilomycin A (35). As expected, cytokine synthesis and expression of costimulatory cell surface molecules induced by cryptococcal DNA was strongly suppressed by these compounds, as they acted on CpG-ODN-induced responses. Furthermore, inhibitory ODN that block the signaling triggered by CpG-ODN in a specific manner (36) suppressed the activation of BM-DCs caused by cryptococcal DNA as well as CpG-ODN. Theses results suggest that Cn DNA was recognized by TLR9 for its capacity to activate BM-DCs, similar to the case of CpG-ODN.

In agreement with this possibility, the effects of cryptococcal DNA required the presence of TLR9, as shown in the present results, in which the production of IL-12p40 and expression of CD40 by BM-DCs stimulated with cryptococcal DNA were cancelled in TLR9$^{-/-}$ mice, similar to the results seen upon the use of CpG-ODN. The TLR9 signaling is dependent on an adaptor molecule, MyD88, but not on TRIF, the latter of which mediates the signals triggered by TLR3 and TLR4 (37). This notion is consistent with our findings of failure of activation of BM-DCs from MyD88$^{-/-}$ mice, but not from TRIF$^{-/-}$ mice, when stimulated by cryptococcal DNA. These results suggest that cryptococcal DNA triggers TLR9 and delivers the activation signals with MyD88. In agreement with this scenario, methylation of cryptococcal DNA led to a reduction in its ability to induce cytokine synthesis by BM-DCs, a treatment known to diminish the activity of CpG-ODN via interaction with TLR9 (16, 24). In addition, using a NF-κB reporter assay, cryptococcal DNA triggered the activation signals in HEK293 transfected with the TLR9 gene. Thus, to our best knowledge, fungal DNA was first found to promote the activation of BM-DCs by triggering the TLR9-dependent and MyD88-mediated signaling pathway. In this study, methylation of cryptococcal DNA did not completely abrogate its ability to stimulate cytokine synthesis by BM-DCs, in contrast to the effect of this treatment on CpG-ODN. Although a possibility that cryptococcal DNA was not completely methylated is not excluded, these data suggest a TLR9-mediated, but CpG-independent activation mechanism for cryptococcal DNA, which may be consistent with the recent observations that TLR9 recognizes DNA not only by the CpG motif but also by different nucleic acid sequences (41).

In the present study, BM-DCs were stimulated by adding cryptococcal DNA to the cell cultures, suggesting that the DNA was internalized through the cell membranes and moved into the endosomal pathway as described previously for CpG-ODN (19, 20). This possibility was confirmed using confocal microscopy performed by comparing the intracellular trafficking of fluorescence-labeled cryptococcal DNA and CpG-ODN. The results showed colocalization of these two nucleic acids throughout the course of incubation. Thus, the intracellular trafficking of cryptococcal ODN to the endosomal pathway is similar to that of the CpG-ODN. Latz et al. (19) demonstrated the redistribution of TLR9 toward the sites of CpG-ODN accumulation. Compatible with this observation, in the present study, redistribution of TLR9 to the sites of cryptococcal DNA accumulation was noted in BM-DCs. These results add further support to our conclusion that cryptococcal DNA activated BM-DCs for cytokine synthesis and expression of costimulatory cell surface molecules by triggering the TLR9 signaling pathway, although we could not confirm that cryptococcal DNA directly binds TLR9.

Based on our findings, we propose here a novel mechanism for recognition of fungal pathogen by the host immune system: the DCs sense Cn DNA in a TLR9-dependent fashion. Cn infects lung tissues and multiplies in alveolar spaces. It has recently been proposed that this fungal pathogen grows inside the endosomes of macrophages based on its escape mechanism against killing effector molecules (1). Macrophages acquire the capacity to kill the fungus after their activation by IFN-γ secreted from Th1 cells (5). Therefore, it is unlikely that the DNA is released from Cn outside the macrophages and DCs, but rather generated from the killed yeast cells in the endosomal compartment, which could be moved into the TLR9-triggered signaling pathway for the initiation of host protective immune responses. Consistent with this notion, activation of BM-DCs by whole cryptococcal cells was significantly, although not completely, reduced in TLR9$^{-/-}$ mice, and these mice were more susceptible to pulmonary infection with Cn than WT control mice, as shown by the increased live colonies in lungs, when Cap67, an acapsular strain, was used. In this regard, it was recently demonstrated that DCs could incorporate and kill this fungal microorganism (42, 43). In our data, the culture supernatants of YC-11, a highly encapsulated Cn, containing much capsular polysaccharides suppressed the production of IL-12p40 by cryptococcal DNA and, in addition, BM-DCs failed to produce IL-12p40 upon stimulation with whole yeast cells of YC-11 in contrast to Cap67 (Fig. 4, *c* and *d*), although DNA from the former strain was as potent as the latter ones (Fig. 1*e*). These observations raise a possibility that capsular polysaccharides interfere with the BM-DC production of IL-12p40 in response to cryptococcal DNA, which may limit the significance of our findings. However, Cn is known to have no capsule or a thin capsule when infected via the airborne route, which may provide a benefit for them to reach the alveolar space (44). This notion suggests that DCs may encounter acapsular

or thinly capsulated Cn and may be activated by DNA released from engulfed yeast cells under little influence of capsular polysaccharides at the early stage of infection. Further investigations are necessary to address this important issue.

Thus, the present findings enhance our understanding of the pathogenic mechanism of intractable cryptococcal infection in immunocompromised patients and help in the design of novel immunotherapies to combat such clinically difficult infection.

Disclosures

The authors have no financial conflict of interest.

References

1. Feldmesser, M., S. Tucker, and A. Casadevall. 2001. Intracellular parasitism of macrophages by *Cryptococcus neoformans*. *Trends Microbiol.* 9: 273–278.
2. Lim, T. S., and J. W. Murphy. 1980. Transfer of immunity to cryptococcosis by T-enriched splenic lymphocytes from *Cryptococcus neoformans*-sensitized mice. *Infect. Immun.* 30: 5–11.
3. Mody, C. H., M. F. Lipscomb, N. E. Street, and G. B. Toews. 1990. Depletion of $CD4^+L3T4^+$ lymphocytes in vivo impairs murine host defense to *Cryptococcus neoformans*. *J. Immunol.* 144: 1472–1477.
4. Hill, J. O., and A. G. Harmsen. 1991. Intrapulmonary growth and dissemination of an avirulent strain of *Cryptococcus neoformans* in mice depleted of $CD4^+$ or $CD8^+$ T cells. *J. Exp. Med.* 173: 755–758.
5. Koguchi, Y., and K. Kawakami. 2002. Cryptococcal infection and Th1-Th2 cytokine balance. *Int. Rev. Immunol.* 21: 423–438.
6. Mansour, M. K., E. Latz, and S. M. Levitz. 2006. *Cryptococcus neoformans* glycoantigens are captured by multiple lectin receptors and presented by dendritic cells. *J. Immunol.* 176: 3053–3061.
7. Lipscomb, M. F., T. Alvarellos, G. B. Toews, R. Tompkins, Z. Evans, G. Koo, and V. Kumar. 1987. Role of natural killer cells in resistance to *Cryptococcus neoformans* infections in mice. *Am. J. Pathol.* 128: 354–361.
8. Kawakami, K., Y. Kinjo, K. Uezu, S. Yara, K. Miyagi, Y. Koguchi, T. Nakayama, M. Taniguchi, and A. Saito. 2001. Monocyte chemoattractant protein-1-dependent increase of Vα14 NKT cells in lungs and their roles in Th1 response and host defense in cryptococcal infection. *J. Immunol.* 167: 6525–6532.
9. Uezu, K., K. Kawakami, K. Miyagi, Y. Kinjo, T. Kinjo, H. Ishikawa, and A. Saito. 2004. Accumulation of γδ T cells in the lungs and their regulatory roles in Th1 response and host defense against pulmonary infection with *Cryptococcus neoformans*. *J. Immunol.* 172: 7629–7634.
10. Mednick, A. J., M. Feldmesser, J. Rivera, and A. Casadevall. 2003. Neutropenia alters lung cytokine production in mice and reduces their susceptibility to pulmonary cryptococcosis. *Eur. J. Immunol.* 33: 1744–1753.
11. Takeda, K., T. Kaisho, and S. Akira. 2003. Toll-like receptors. *Annu. Rev. Immunol.* 21: 335–376.
12. Yauch, L. E., M. K. Mansour, S. Shoham, J. B. Rottman, and S. M. Levitz. 2004. Involvement of CD14, Toll-like receptors 2 and 4, and MyD88 in the host response to the fungal pathogen *Cryptococcus neoformans* in vivo. *Infect. Immun.* 72: 5373–5382.
13. Biondo, C., A. Midiri, L. Messina, F. Tomasello, G. Garufi, M. R. Catania, M. Bombaci, C. Beninati, G. Teti, and G. Mancuso. 2005. MyD88 and TLR2, but not TLR4, are required for host defense against *Cryptococcus neoformans*. *Eur. J. Immunol.* 35: 870–878.
14. Nakamura, K., K. Miyagi, Y. Koguchi, Y. Kinjo, K. Uezu, T. Kinjo, M. Akamine, J. Fujita, I. Kawamura, M. Mitsuyama, et al. 2006. Limited contribution of Toll-like receptor 2 and 4 to the host response to a fungal infectious pathogen, *Cryptococcus neoformans*. *FEMS Immunol. Med. Microbiol.* 47: 148–154.
15. Shoham, S., C. Huang, J. M. Chen, D. T. Golenbock, and S. M. Levitz. 2001. Toll-like receptor 4 mediates intracellular signaling without TNF-α release in response to *Cryptococcus neoformans* polysaccharide capsule. *J. Immunol.* 166: 4620–4626.
16. Krieg, A. M., A. K. Yi, S. Matson, T. J. Waldschmidt, G. A. Bishop, R. Teasdale, G. A. Koretzky, and D. M. Klinman. 1995. CpG motifs in bacterial DNA trigger direct B-cell activation. *Nature* 374: 546–549.
17. Krieg, A. M. 2002. CpG motifs in bacterial DNA and their immune effects. *Annu. Rev. Immunol.* 20: 709–760.
18. Hemmi, H., O. Takeuchi, T. Kawai, T. Kaisho, S. Sato, H. Sanjo, M. Matsumoto, K. Hoshino, H. Wagner, K. Takeda, and S. Akira. 2000. A Toll-like receptor recognizes bacterial DNA. *Nature* 408: 740–745.
19. Latz, E., A. Schoenemeyer, A. Visintin, K. A. Fitzgerald, B. G. Monks, C. F. Knetter, E. Lien, N. J. Nilsen, T. Espevik, and D. T. Golenbock. 2004. TLR9 signals after translocating from the ER to CpG DNA in the lysosome. *Nat. Immunol.* 5: 190–198.
20. Honda, K., Y. Ohba, H. Yanai, H. Negishi, T. Mizutani, A. Takaoka, C. Taya, and T. Taniguchi. 2005. Spatiotemporal regulation of MyD88-IRF-7 signalling for robust type-I interferon induction. *Nature* 434: 1035–1040.
21. Kawai, T., S. Sato, K. J. Ishii, C. Coban, H. Hemmi, M. Yamamoto, K. Terai, M. Matsuda, J. Inoue, S. Uematsu, et al. 2004. Interferon-α induction through Toll-like receptors involves a direct interaction of IRF7 with MyD88 and TRAF6. *Nat. Immunol.* 5: 1061–1068.
22. Brown, W. C., D. M. Estes, S. E. Chantler, K. A. Kegerreis, and C. E. Suarez. 1998. DNA and a CpG oligonucleotide derived from *Babesia bovis* are mitogenic for bovine B cells. *Infect. Immun.* 66: 5423–5432.
23. Shoda, L. K., K. A. Kegerreis, C. E. Suarez, I. Roditi, R. S. Corral, G. M. Bertot, J. Norimine, and W. C. Brown. 2001. DNA from protozoan parasites *Babesia bovis*. *Trypanosoma cruzi*, and *T. brucei* is mitogenic for B lymphocytes and stimulates macrophage expression of interleukin-12, tumor necrosis factor α, and nitric oxide. *Infect. Immun.* 69: 2162–2171.
24. Sun, S., C. Beard, R. Jaenisch, P. Jones, and J. Sprent. 1997. Mitogenicity of DNA from different organisms for murine B cells. *J. Immunol.* 159: 3119–3125.
25. Souza, M. C., M. Correa, S. R. Almeida, J. D. Lopes, and Z. P. Camargo. 2001. Immunostimulatory DNA from *Paracoccidioides brasiliensis* acts as T-helper 1 promoter in susceptible mice. *Scand. J. Immunol.* 54: 348–356.
26. Yamamoto, M., S. Sato, H. Hemmi, K. Hoshino, T. Kaisho, H. Sanjo, O. Takeuchi, M. Sugiyama, M. Okabe, K. Takeda, and S. Akira. 2003. Role of adaptor TRIF in the MyD88-independent Toll-like receptor signaling pathway. *Science* 301: 640–643.
27. Adachi, O., T. Kawai, K. Takeda, M. Matsumoto, H. Tsutsui, M. Sakagami, K. Nakanishi, and S. Akira. 1998. Targeted disruption of the MyD88 gene results in loss of IL-1- and IL-18-mediated function. *Immunity* 9: 143–150.
28. Saijo, S., N. Fujikado, T. Furuta, H. Kotaki, K. Seki, K. Sudo, S. Akira, Y. Adachi, N. Ohno, T. Kinjo, et al. 2007. Dectin-1 plays an important role in the host defense mechanism against pathogenic fungus *Pneumocystis carinii* under immuno-compromised conditions. *Nat. Immunol.* 8: 39–46.
29. Yasuoka, A., S. Kohno, H. Yamada, M. Kaku, and H. Koga. 1994. Influence of molecular sizes of *Cryptococcus neoformans* capsular polysaccharide on phagocytosis. *Microbiol. Immunol.* 38: 851–856.
30. Ishibashi, K., N. Miura, Y. Adachi, N. Ogura, H. Tamura, S. Tanaka, and N. Ohno. 2004. DNA array analysis of altered gene expression in human leukocytes stimulated with soluble and particulate forms of *Candida* cell wall β-glucan. *Int. Immunopharmacol.* 4: 387–401.
31. Lutz, M. B., N. Kukutsch, A. L. Ogilvie, S. Rossner, F. Koch, N. Romani, and G. Schuler. 1999. An advanced culture method for generating large quantities of highly pure dendritic cells from mouse bone marrow. *J. Immunol. Methods* 223: 77–92.
32. Chuang, T. H., J. Lee, L. Kline, J. C. Mathison, and R. J. Ulevitch. 2002. Toll-like receptor 9 mediates CpG-DNA signaling. *J. Leukocyte Biol.* 71: 538–544.
33. Monari, C., F. Bistoni, and A. Vecchiarelli. 2006. Glucuronoxylomannan exhibits potent immunosuppressive properties. *FEMS Yeast Res.* 6: 537–542.
34. Gantner, B. N., R. M. Simmons, S. J. Canavera, S. Akira, and D. M. Underhill. 2003. Collaborative induction of inflammatory responses by dectin-1 and Toll-like receptor 2. *J. Exp. Med.* 197: 1107–1117.
35. Hacker, H., H. Mischak, T. Miethke, S. Liptay, R. Schmid, T. Sparwasser, K. Heeg, G. B. Lipford, and H. Wagner. 1998. CpG-DNA-specific activation of antigen-presenting cells requires stress kinase activity and is preceded by non-specific endocytosis and endosomal maturation. *EMBO J.* 17: 6230–6240.
36. Stunz, L. L., P. Lenert, D. Peckham, A. K. Yi, S. Haxhinasto, M. Chang, A. M. Krieg, and R. F. Ashman. 2002. Inhibitory oligonucleotides specifically block effects of stimulatory CpG oligonucleotides in B cells. *Eur. J. Immunol.* 32: 1212–1222.
37. Akira, S., and K. Takeda. 2004. Toll-like receptor signalling. *Nat. Rev. Immunol.* 4: 499–511.
38. Alexopoulou, L., A. C. Holt, R. Medzhitov, and R. A. Flavell. 2001. Recognition of double-stranded RNA and activation of NF-κB by Toll-like receptor 3. *Nature* 413: 732–738.
39. Hemmi, H., T. Kaisho, O. Takeuchi, S. Sato, H. Sanjo, K. Hoshino, T. Horiuchi, H. Tomizawa, K. Takeda, and S. Akira. 2002. Small anti-viral compounds activate immune cells via the TLR7 MyD88-dependent signaling pathway. *Nat. Immunol.* 3: 196–200.
40. Vollmer, J., S. Tluk, C. Schmitz, S. Hamm, M. Jurk, A. Forsbach, S. Akira, K. M. Kelly, W. H. Reeves, S. Bauer, and A. M. Krieg. 2005. Immune stimulation mediated by autoantigen binding sites within small nuclear RNAs involves Toll-like receptors 7 and 8. *J. Exp. Med.* 202: 1575–1585.
41. Vollmer, J., R. D. Weeratna, M. Jurk, U. Samulowitz, M. J. McCluskie, P. Payette, H. L. Davis, C. Schetter, and A. M. Krieg. 2004. Oligodeoxynucleotides lacking CpG dinucleotides mediate Toll-like receptor 9 dependent T helper type 2 biased immune stimulation. *Immunology* 113: 212–223.
42. Syme, R. M., J. C. Spurrell, E. K. Amankwah, F. H. Green, and C. H. Mody. 2002. Primary dendritic cells phagocytose *Cryptococcus neoformans* via mannose receptors and Fcγ receptor II for presentation to T lymphocytes. *Infect. Immun.* 70: 5972–5981.
43. Wozniak, K. L., J. M. Vyas, and S. M. Levitz. 2006. In vivo role of dendritic cells in a murine model of pulmonary cryptococcosis. *Infect. Immun.* 74: 3817–3824.
44. Powell, K. E., B. A. Dahl, R. J. Weeks, and F. E. Tosh. 1972. Airborne *Cryptococcus neoformans*: particles from pigeon excreta compatible with alveolar deposition. *J. Infect. Dis.* 125: 412–415.

Potent Antimycobacterial Activity of Mouse Secretory Leukocyte Protease Inhibitor[1]

Junichi Nishimura,*§ Hiroyuki Saiga,*‡ Shintaro Sato,¶ Megumi Okuyama,‖ Hisako Kayama,*‡ Hirotaka Kuwata,* Sohkichi Matsumoto,‖ Toshirou Nishida,§ Yoshiki Sawa,§ Shizuo Akira,¶ Yasunobu Yoshikai,† Masahiro Yamamoto,‡ and Kiyoshi Takeda[2]*‡

Secretory leukocyte protease inhibitor (SLPI) has multiple functions, including inhibition of protease activity, microbial growth, and inflammatory responses. In this study, we demonstrate that mouse SLPI is critically involved in innate host defense against pulmonary mycobacterial infection. During the early phase of respiratory infection with *Mycobacterium bovis* bacillus Calmette-Guérin, SLPI was produced by bronchial and alveolar epithelial cells, as well as alveolar macrophages, and secreted into the alveolar space. Recombinant mouse SLPI effectively inhibited in vitro growth of bacillus Calmette-Guérin and *Mycobacterium tuberculosis* through disruption of the mycobacterial cell wall structure. Each of the two whey acidic protein domains in SLPI was sufficient for inhibiting mycobacterial growth. Cationic residues within the whey acidic protein domains of SLPI were essential for disruption of mycobacterial cell walls. Mice lacking SLPI were highly susceptible to pulmonary infection with *M. tuberculosis*. Thus, mouse SLPI is an essential component of innate host defense against mycobacteria at the respiratory mucosal surface. *The Journal of Immunology*, 2008, 180: 4032–4039.

Mycobacterium tuberculosis is a top killer among bacterial pathogens and is responsible for 2 million deaths annually. The emergence of AIDS and development of multidrug-resistant *M. tuberculosis* have increased the incidence of tuberculosis, and it has now become a serious problem. Therefore, the host defense mechanisms against *M. tuberculosis* have been intensively investigated and important roles of T cell-mediated adaptive immunity are now well established (1, 2). In addition, functional characterization of TLRs has recently indicated the importance of innate immunity in infection with *M. tuberculosis* (3, 4). Macrophages and dendritic cells are the major effectors of TLR-mediated antimycobacterial immune responses, because they produce a variety of proinflammatory cytokines and have the capacity of phagocytosis. However, during *M. tuberculosis* infection, epithelial cells in the respiratory tract as well as alveolar macrophages are the first targets for invasion by *M. tuberculosis*. Therefore, these epithelial cells are expected to play roles in preventing mycobacterial infection by establishing physical barriers and producing proinflammatory and antimicrobial mediators (5).

Secretory leukocyte protease inhibitor (SLPI)[3] is a 12-kDa secreted protein composed of two cysteine-rich whey acidic protein (WAP) domains (also called WAP four-disulfide core (WFDC) domains) (6–8). It was originally identified in seminal fluid and is produced by secretory cells in the genital, respiratory, and lacrimal glands as well as dermal keratinocytes (9–13). SLPI is a potent inhibitor of serine proteases, such as neutrophil elastase and cathepsin G, and has therefore been proposed to protect tissues from protease-mediated damage at sites of inflammation (14, 15). Indeed, SLPI was subsequently shown to mediate wound healing (16, 17). Further studies have revealed that SLPI has additional functions. For example, it possesses an antimicrobial activities against Gram-negative and Gram-positive bacteria, fungi, and viruses, including HIV (18–20). In addition to SLPI, several other serine protease inhibitors containing a single WAP domain, such as Eppin, Elafin, SWAM1, and SWAM2, also possess antimicrobial activities against Gram-negative and Gram-positive bacteria (8, 21, 22). Thus, serine protease inhibitors possessing WAP domains exhibit antimicrobial activities. However, the precise mechanisms by which these serine protease inhibitors exert their antimicrobial activities remain elusive. More recently, SLPI was found to mediate anti-inflammatory responses. Briefly, SLPI is induced in monocytes and macrophages in response to inflammatory stimuli mediated by TLRs (23) and subsequently suppresses TLR-dependent production of inflammatory mediators in macrophages by modulating NF-κB activity (23–25). Consistent with these findings, SLPI-deficient mice are highly sensitive to TLR4 ligand (LPS)-induced endotoxin shock with increased production of IL-6 (26). Thus, SLPI has diverse functions and its precise roles need to be investigated more carefully.

*Deparment of Molecular Genetics and †Division of Host Defense, Research Center for Prevention of Infectious Diseases, Medical Institute of Bioregulation, Kyushu University, Fukuoka; ‡Laboratory of Immune Regulation, Department of Microbiology and Immunology, §Department of Surgery, Graduate School of Medicine, and ¶Department of Host Defense, Research Institute for Microbial Diseases, Osaka University; and ‖Department of Host Defense, Osaka City University Graduate School of Medicine, Osaka, Japan

Received for publication April 3, 2007. Accepted for publication January 9, 2008.

The costs of publication of this article were defrayed in part by the payment of page charges. This article must therefore be hereby marked *advertisement* in accordance with 18 U.S.C. Section 1734 solely to indicate this fact.

[1] This work was supported by a Grant-in-Aid from the Ministry of Education, Culture, Sports, Science and Technology and the Ministry of Health, Labor and Welfare, as well as the Tokyo Biochemical Research Foundation, the Cell Science Research Foundation, the Yakult Bio-Science Foundation, the Osaka Foundation for Promotion of Clinical Immunology, the Sumitomo Foundation, and the Sankyo Foundation of Life Science.

[2] Address correspondence and reprint requests to Dr. Kiyoshi Takeda, Laboratory of Immune Regulation, Department of Microbiology and Immunology, Graduate School of Medicine, Osaka University, Suita, Osaka, 565-0871, Japan. E-mail address: ktakeda@ongene.med.osaka-u.ac.jp

[3] Abbreviations used in this paper: SLPI, secretory leukocyte protease inhibitor; WAP, whey acidic protein; WFDC, WAP four-disulfide core; qPCR, quantitative PCR; BALF, bronchoalveolar lavage fluid; BCG, bacillus Calmette-Guérin; FLUOS, 5-(6-)carboxyfluorescein-*N*-hydroxysuccinimide ester; NPN, 1-*N*-phenylnapthylamine; AEC, alveolar epithelial cell.

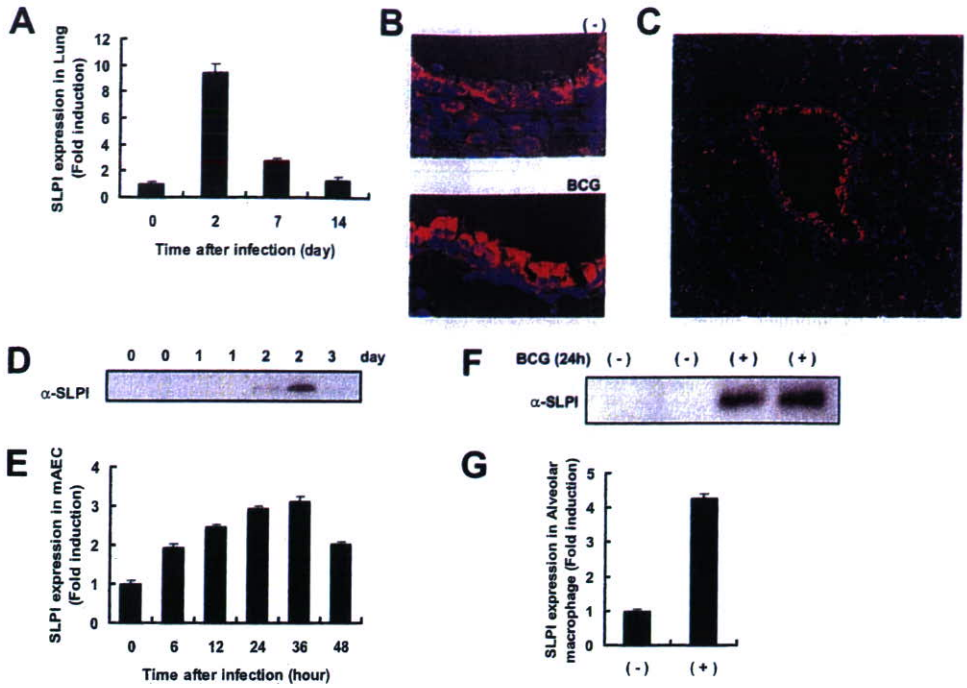

FIGURE 1. Expression of SLPI during mycobacterium infection. *A*, Wild-type mice were intratracheally infected with BCG (4×10^5 CFU). At the indicated periods, total RNA was extracted from the lungs. SLPI mRNA expression was analyzed by quantitative real-time RT-PCR. Data are shown as the relative mRNA levels normalized by the corresponding 18S rRNA level. *B* and *C*, At 2 days after intratracheal infection with BCG, lung tissue sections were stained with an anti-SLPI Ab (red) and 4′,6-diamidino-2-phenylindole (blue) and visualized by fluorescence microscopy. *D*, BALF was collected at the indicated periods after BCG infection. Mouse SLPI protein expression was analyzed by Western blotting with an anti-SLPI Ab. Data obtained from two independent mice (0, 1, and 2 days) are indicated. *E*, AEC were incubated with the same number of BCG for the indicated periods. SLPI mRNA expression was analyzed by quantitative real-time RT-PCR. Data are shown as the relative mRNA levels normalized by the corresponding 18S rRNA level. *F*, AEC were incubated with the same number of BCG. Culture supernatants were collected before (−) and after 24 h of infection (+) and subjected to Western blot analysis using an anti-SLPI Ab. Data obtained from two independent cell clones are shown. *G*, Alveolar macrophages were collected from uninfected wild-type mice, cultured with or without BCG for 48 h, and then analyzed for their SLPI mRNA expression by quantitative real-time RT-PCR. The results are presented as the mean ± SD.

In this study, we investigated the roles of murine SLPI in the context of host defenses against mycobacteria, since SLPI expression is greatly induced in macrophages and the lungs during mycobacterial infection (27). Recombinant SLPI inhibited mycobacterial growth at a lower concentration than that required to inhibit bacterial growth. Inhibition of mycobacterial growth was mediated by increased permeability of the mycobacterial membrane. Mutation of cationic residues in the WAP domains of SLPI resulted in loss of its antimycobacterial activity. Furthermore, SLPI-deficient mice were highly susceptible to pulmonary infection with *M. tuberculosis*. These findings demonstrate that SLPI is a potent antimycobacterial molecule.

Materials and Methods

Cells and bacteria

M. tuberculosis strains H37Ra (ATCC 25177; American Type Culture Collection) and *M. tuberculosis* strains H37Rv (28) were grown in Middlebrook 7H9-ADC medium for 2 wk and stored at −80°C until use. *Mycobacterium bovis* bacillus Calmette-Guérin (BCG; Tokyo strain) was purchased from Kyowa Pharmaceuticals. *Salmonella enterica* serovar *typhimurium* were provided by the Research Institute for Microbial Diseases (Osaka University). For each experiment, the dose was confirmed by plating an aliquot of the injected bacterial suspension. Isolation and immortalization of type II alveolar epithelial cells from the lungs of transgenic H-2K^b-tsA58 mice were performed as previously described (29), with some modifications.

Immunohistochemistry

Lungs were washed with PBS and frozen in Tissue-Tex OCT compound (Sakura, Tokyo, Japan). Cryostat sections (5-μm thick) were fixed with cold acetone for 10 min, dried, rehydrated with PBS, and blocked with PBS containing 20 mM HEPES, 10% FBS, and 1 μg of Fc-blocking mAb (2.4G2; BD Pharmingen). Next, the sections were sequentially incubated with a biotinylated anti-mouse SLPI Ab (R&D Systems) and Alexa Fluor 594-conjugated streptavidin (Molecular Probes). The nuclei were stained with 4′,6-diamidino-2-phenylindole (Molecular Probes). After washing with PBS, the sections were analyzed by confocal microscopy (Zeiss).

Western blot analysis

Samples were boiled for 5 min in reducing SDS-PAGE sample buffer and then subjected to SDS-PAGE. The separated proteins were transferred to a 0.45-μm pore polyvinylidene fluoride membrane (Millipore). After blocking with 5% milk, the membrane was incubated with the above-described biotinylated anti-mouse SLPI Ab (0.2 μg/ml) and a streptavidin-HRP complex (1/10,000 dilution; R&D Systems). The bound Abs were detected by the Super Signal reagent (Pierce).

Quantitative real-time RT-PCR

After isolation of total RNA with the TRIzol reagent (Invitrogen Life Technologies), 4 μg of the RNA was treated with RQ1DNase (Promega) and then reverse-transcribed using Moloney murine leukemia virus reverse transcriptase (Promega) and Random Primers (Toyobo). Gene expression was quantified with an Applied Biosystems PRISM 7000 sequence detection system using TaqMan Universal PCR Master Mix (Applied Biosystems). To determine the relative expression level of each sample, the corresponding 18S rRNA expression level was measured as an internal control. The primer and probe sequences for SLPI were follows: quantitative PCR (qPCR) primer (forward), 5′-d(GCTGTGAGGGTATATGTG GGAAA)-3′; qPCR primer (reverse), 5′-d(CGCCAATGTCAGGGAT CAG)-3′; and qPCR probe, 5′-FAMd(TCTGCCTGCCCCCGATGTG AG)BHQ-3′.